2019

Analysis of the Molecular Mechanisms Governing FCγ Receptor Activation on the Surfaces of Macrophages by Advanced Optical Microscopy

Elizabeth Michelle Bailey
South Dakota State University

ANALYSIS OF THE MOLECULAR MECHANISMS GOVERNING FCγ RECEPTOR ACTIVATION ON THE SURFACES OF MACROPHAGES BY ADVANCED OPTICAL MICROSCOPY

BY

ELIZABETH MICHELLE BAILEY

A dissertation submitted in partial fulfillment of the requirements for the

Doctor of Philosophy

Major in Biochemistry

South Dakota State University

2019

DISSERTATION ACCEPTANCE PAGE

ELIZABETH MICHELLE BAILEY

This dissertation is approved as a creditable and independent investigation by a candidate for the Doctor of Philosophy degree and is acceptable for meeting the dissertation requirements for this degree. Acceptance of this does not imply that the conclusions reached by the candidate are necessarily the conclusions of the major department.

Adam D. Hoppe, Ph.D
Advisor Date

Douglas Raynie
Department Head Date

Dean, Graduate School Date

ACKNOWLEDGMENTS

I would first like to offer sincere gratitude to my advisor, Dr. Adam Hoppe, for seeing potential in me and challenging me every step of the way while being a source of support and encouragement. I would also like to thank all the past and present lab members for their constant support and inspiration. I would like to specifically extend gratitude to our past lab member Dr. Brandon Scott for his mentorship.

I am especially grateful for my parents, whom I wish could be here to flip through these pages and see what I have accomplished. Their unending selflessness made it possible for me to follow my passion to its fullest extent. I could not have done this without their unwavering faith in me and constant encouragement.

Much appreciation goes to two of the strongest, most independent women I know, my two grandmothers, Betty Mikesell and Beverly Bailey, who instilled a great work ethic, appreciation for life-long learning, and at times, and a little fear of authority. Thanks to my many siblings for being my long-distance cheerleaders throughout this process, and some of the hardest moments of life so far. Sierra and Savannah, my twin pillars (in both the literal and metaphorical sense), I have appreciated the long phone calls for encouragement and sardonic humor to decompress throughout this journey.

There is one more amazing woman and friend I would be remiss to leave out, my much cooler, lifelong friend, Tonia. Your enduring friendship is one of my most cherished possessions and has impacted me in more ways than I can describe.

Khaj and Rosie, my two longest standing roommates, thank you for always making sure I was up and ready for a new day in the lab, whether you guys let me sleep well the night before or not. These two characters have brought so much to my life.

Lastly, I must acknowledge my best friend and ally in all of life's adventures, Eric, for his unwavering support, kindness, and encouragement. Thank you for seeing what I was capable of and convincing me to do the same. You helped make this possible.

The work in chapter three was funded by a research sponsorship from Momenta Pharmaceuticals. The author nor the mentor, Adam Hoppe, do not hold stock or were compensated by the company. This material is based on work supported by National Science Foundation/EPSCoR award No. IIA-1355423 and by the state of South Dakota's Governor's Office of Economic Development as a South Dakota Research Innovation Center (SDRIC). *Any opinions, findings, and conclusions or recommendations expressed in this material are those of the author(s) and do not necessarily reflect the views of the National Science Foundation.*

TABLE OF CONTENTS

LIST OF FIGURES

ABSTRACT

ANALYSIS OF THE MOLECULAR MECHANISMS GOVERNING FCγ RECEPTOR ACTIVATION ON THE SURFACES OF MACROPHAGES BY ADVANCED OPTICAL MICROSCOPY

ELIZABETH MICHELLE BAILEY

2019

Therapeutic antibodies are achieving new levels of therapeutic success in treating cancers and immunological disorders by antibody engagement of Fc receptor-directed immune responses. Conversely, inhibiting autoantibody induced Fc receptor activation is an attractive approach to treat autoimmune diseases. Immunoglobulin G (IgG) antibodies are often the principal subclass used in therapeutic antibodies and associated with autoimmune pathologies because of their long circulation and potent effector functions, including activation of the Fcγ Receptor (FcγR). Thus, a thorough understanding of the FcγR activation is required to improve the efficacy of immunotherapies and to mitigate autoimmunities. It is well established that FcγR clustering is required for activation, yet the minimum number of FcγRs and the spatial characteristics of this activation remain incompletely understood. In this dissertation, sophisticated microscopy methods were employed to elucidate how IgG binding to FcγRs changes their diffusion, membrane topographical environment and the recruitment of the essential kinase Syk. Additionally, this dissertation uses single particle tracking methods (SPT) to examine FcγR cluster valency and activation. Major findings from this work include demonstration that clustering of five FcγRs is sufficient for activation on endosomes, but not the plasma membrane. The findings of this dissertation also provide insights into the mechanisms of

action of an FcγR inhibitor for IgG-mediated autoimmune diseases that binds three FcγRs. Together, this work represents significant new insights into FcγR activation that may contribute to the field of basic immunology and may impact immunotherapy design strategy.

CHAPTER I. INTRODUCTION

Immune cells, working in concert must integrate an intricate network of activating and inhibitory signals to regulate the innate and adaptive immune responses. Pro-inflammatory signals ensue when the scales are tipped in the direction of activating signals. Effective responses of this pro-inflammatory signaling result in the elimination of invading pathogens such as bacteria or viruses [1]. When inhibitory signals prevail, immune cells are inactive or anti-inflammatory. A major player in this balancing act is the Fcγ receptor (FcγR), which binds to the crystallizable fragment (Fc) of immunoglobulin G (IgG) antibodies that are attached to antigens, on the surface of a target, by their variable fragments (Fv). FcγR binding to antibody-antigen complexes, is essential for IgG-dependent effector functions. Activating and inhibitory FcγRs are expressed across innate and adaptive immune cells including dendritic cells, neutrophils, and macrophages, whereas, inhibitory FcγR is expressed on B cells, where it regulates IgG affinity maturation and production. The roles of the FcγR vary widely and include phagocytosis, activation of natural killer cells and regulating antibody production in B cells [2, 3]. In macrophages, FcγR signaling results ins phagocytosis [3], ADCC, and the release of pro-inflammatory cytokines [2].

Together, these FcγR effector functions define both activating and inhibitory activities of the innate and adaptive immune system. In cases of autoimmunity, such as rheumatoid arthritis and systemic lupus erythematosus (SLE), excessive activation of the FcγR by IgG recognizing self-antigen contributes to pro-inflammatory responses characteristic of autoimmune pathogenesis [1, 4, 5]. Manipulation of FcγR activation is

an attractive option for immunotherapies that range from treatment of cancer to autoimmune diseases [1, 6]. Achieving this goal requires a thorough understanding of the mechanisms of FcγR activation and inhibition.

The FcγR family

The human FcγR family (Fig. 1.1) is made up of activating and inhibitory receptors. The activating receptors, FcγRI, FcγRIIa, FcγRIIc, and FcγRIIIa signal using an intracellular domain containing an immunoreceptor tyrosine-based activation motifs (ITAMs). The inhibitory FcγR, FcγRIIb, contains an immunoreceptor tyrosine-based inhibition motifs (ITIMs). The ITAMs for the FcγRIIa and FcγRIIc are located on their cytoplasmic tail while the FcγRI and FcγRIIIa have ITAMs within an associated dimer referred to as the common gamma chain (FcRγ, Fig. 1.1). The FcRγ is common to the FcεRI, and is shared among the other activating FcRs, (FcγRI, FcγRIIIa, and FcαRI) as well as other immune receptors (GPVI, OSCAR, TREM) and activates a wide array of immune functions [7, 8].

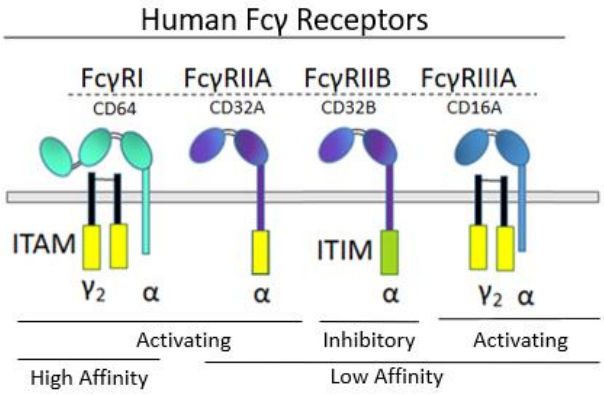

Figure 1.1 The FcγR Family. A) The FcγR family members are made up of activating and inhibitory receptors that vary in affinity, with FcγRI being the high affinity receptor for IgG1.

All the FcγRs have extracellular domains comprised of multiple IgG-domains. The three IgG like domains of FcγRI, the high affinity receptor, enable it to bind IgG with Ka~10^9. The high affinity receptor, FcγRI, or CD64, is the most studied of the FcγRs. Association of the FcγR with the FcRγ occurs through salt bridges between the acidic residues of the signaling dimer and the basic amino acids of the receptor within the transmembrane region [9]. FcγRI also associates with the FcRγ via interactions between aromatic and polar residues that span the length of the transmembrane domain [10].

ITAMs, Receptor Activation, Signaling

A common feature across immune receptors such as the FcγR, T cell receptor (TCR), B cell receptor (BCR), and the FcεR, is that receptor cross-linking, also referred to as clustering, is required for activation and successful signaling propagation. Upon engagement of the FcγR with an antibody-opsonized target, receptors undergo clustering [11]. In the T and B cell receptors, receptors cluster and accumulate at the central super molecular activation complex (cSMAC). The receptor clustering at the cSMAC creates a narrow synapse between the cell and its target that excludes tall phosphatases [12-14]. Exclusion of phosphatases facilitate ITAM proximity of ITAMs for signal amplification via Syk kinase [11, 15]. Currently, it is thought that FcγR clustering is associated with integrins that form a physical barrier between phosphatases, like CD45, and the clustered receptors at the phagocytic cup [16]. Clustered FcγRs provoke phosphorylation of the ITAM's tyrosines by Src Family Kinase, Lyn. The ITAM's phosphorylated tyrosines recruit Syk kinase, where it docks via its tandem SH2 domains [1, 17, 18]. Syk kinase continues to amplify signal by phosphorylating its ten tyrosines that function as autophosphorylation sites [18].

In opposition to the activating signal, inhibitory signaling occurs when FcγRIIb engages adjacent activating FcRs or the B Cell Receptor (BCR), which prompts the ITIM to recruit SHIP or SHIP-1, SH2 domain-containing phosphatases. These negatively regulate the inflammatory responses by dephosphorylating local phosphorylated ITAMs [1, 19].

Syk family kinases: Syk, Zap 70

The T cell receptor (TCR), B cell receptor (BCR), and the FcRs all activate in a similar manner where receptors cross-link and Src family kinases phosphorylate the tyrosines of an ITAM. The tandem phosphorylated ITAMs recruits either Syk kinase, in the case of BCRs and FcRs, and Zap70 in TCRs, where they bind via their two tandem Src homology 2 (SH2) domains. Zap70 is entirely dependent on Src family kinases, where Syk can phosphorylate the ITAMs itself [18].

In addition to two SH2 domains, Syk kinases have a kinase domain that is inactive in the resting state. It is activated by binding both SH2 domains to dually phosphorylated tyrosines. The phosphorylation of tyrosine residues within its interdomain allows kinase activation in the absence of phosphorylated ITAMs. Because of this, Syk has been thought of as a logic switch ("OR") for activation [18].

Syk kinase and its T-lymphocyte homolog, Zap70, have been shown to act differently. This is illustrated across the different immune receptors and will be highlighted by reviewing the function of a significant tyrosine, Tyr130 in Syk and Tyr126 in Zap70, and how differently its role is between the receptors. In BCRs, Tyr130 is responsible for dissociation of Syk from the ITAM and is thought to play an inhibitory

role as a mutation to phosphomimetic glutamate increased kinase activity [18]. For FcεRI, cycling of autophosphorylation and dephosphorylation of Tyr130 of Syk is necessary for amplification of kinase signaling for downstream pathways. When substituted with Glut30, the binding off rate to the ITAM increased, a loss of site-specific Syk autophosphorylation occurred, and downstream signaling and resulting functions such as degranulation and cytokine production were deficient [20]. In the TCR, there is a proposed "catch and release" mechanisms that describes a transient Zap70 kinase recruitment, activation, and translocation to plasma membrane associated protein islands to activate other signaling molecules. The release of Zap70 to the plasma membrane is regulated by Tyr126 [21]. It is possible that this "catch and release" mechanism is employed in other membrane associated pathways and could explain the need for longer binding time of Syk:FcεRI. Syk kinase activity at the ITAMs of the FcγR has not been explored in this capacity, but it is likely to have similarities given that the FcRγ is shared with FcεRI.

Downstream Signaling Pathways

When the FcγR activating signal dominates, a signaling cascade ensues that is responsible for effector functions such as antibody-dependent cell-mediated cytotoxicity (ADCC), oxidative burst, phagocytosis, stimulation of B cell to produce antibodies, and degranulation [1-3, 22]. The cascade of events includes Syk kinase recruitment mediated activation of multiple signaling pathways and downstream effects specific to the cell type (Fig 1.2). In macrophages, Syk activates multiple signal transduction molecules, such as son of sevenless (SOS) and phosphoinositide 3-kinase (PI3K) which catalyzes the conversion of PIP_2 (Phosphatidylinositol 4,5-bisphosphate) to phosphatidylinositol-3,4,5-

trisphosphate (PtdIns(3,4,5)P_3),or PIP_3 [2, 19, 23]. This conversion produces docking sites for Pleckstrin homology (PH) domain containing proteins that include PLCγ (phosphorylates phospholipase Cγ), Gab2, Akt, Bruton's tyrosine kinase (Btk) [23]. Btk phosphorylates phospholipase Cγ. Phospholipase Cγ then hydrolyzes PIP_2 to produce IP3 (inositol triphosphate) and DAG (diacylglycerol) [23]. IP3 migration to the IP3 receptors in the endoplasmic reticulum triggers an increase in intracellular calcium levels, triggering more downstream calcium-dependent channels. An increase in DAG and calcium ions activates the Protein Kinase C (PKC) pathway [24]. An influx of calcium drives PKC activation also promotes downstream responses that include cytokine production and degranulation [23]. In addition to triggering the PLCγ pathway, Btk activates the Rac pathway, which in turn activates the Rho pathway [2]. Another activator of Rac is the guanine nucleotide exchange factor (GEF), Vav, which also is phosphorylated by Syk [23]. The Rac/Rho pathway, made up of Rho small GTPases, is responsible for the signaling needed to regulate the actin dynamic and as a result are responsible for the actin deformation during phagocytosis. Meanwhile, activated SOS triggers activation of the Ras pathway. The Rho, Ras, and PKC pathways in turn induce activation of even more signaling pathways, including MAPK/ERK. These pathways culminate in the control of ADCC, cytokine release, phagocytosis, and oxidative burst [2].

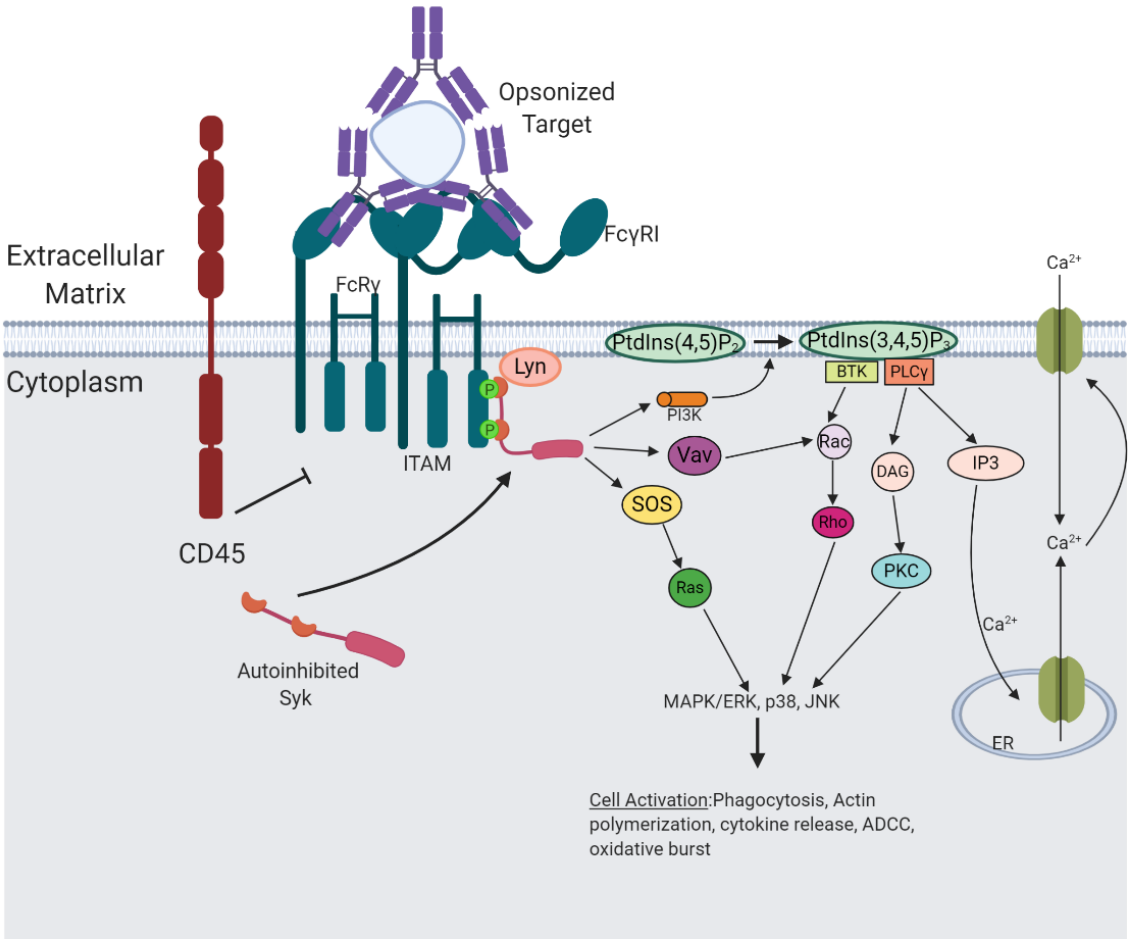

Figure 1.2 Activated FcγR signaling pathway. Clustering of FcγRI by a polyvalent opsonized target activates a phosphorylation cascade that starts with the Src family kinase, Lyn, phosphorylating the two tyrosines of the FcRγ's ITAMs. These phosphotyrosines recruit Syk kinase, causing it to exit its autoinhibited state and to dock its tandem SH2 domains to the phosphotyrosines. Syk then continues to autophosphorylate its 10 tyrosines (not illustrated here for simplicity) as well as PI3K, Vav, and SOS. PIP_3 production recruits Btk and PLCγ, which activates other downstream kinases and GTPases and cause an influx of calcium ions. These go on to activate many other pathways, which culminate in actin cytoskeleton reformation, phagocytosis, cytokine release, oxidative burst and ADCC. (Created with BioRender)

The inflammatory response and FcγR autoimmunity

Understanding the FcγR in the context of macrophages is of high interest, as they are powerful phagocytes that reside in all organs and tissues and play a role in both innate and adaptive immunity. In a general inflammatory response, such as an infected wound,

PAMPs, DAMPS, and kinins are present as a result of invading microorganisms and damaged host cells. The kinins increase blood flow and capillaries become leaky so that platelets can make their way to the site of injury. Meanwhile, resident macrophages of the tissue recognize the PAMPs/DAMPs and become activated, causing them to release pro-inflammatory cytokines such as TNF, IL-1, (IFNα in the case of virus and IFNγ, in case of bacterial infection) and IL-6 [18, 25]. Activated macrophages, among other monocytes, lymphocytes, and endothelial cells, release chemokines such as CXCL8 which recruits more immune cells to extravasate through the blood vessel wall to the site of infection [25].

Once activated, macrophages increase their ability to phagocytose efficiently and present antigenic peptides on MHC class II molecules to engage T helper cells. Their role as an antigen presenter is to amplify the adaptive immune response by activating memory or effector T cells at the site of inflammation. The effector cells release IFNγ to hyperactivate the macrophage, which release cytokines to prompt T helper cell differentiation and upregulate the expression of MHC class II molecules on other antigen presenting cells, such as dendritic cells [2, 22, 25]. Thus the uptake of antigen, via antibodies initiates and sustains positive feedback with T helper cells that amplifies the immune response.

As residents of all organs and tissues, macrophages are well positioned for clearing foreign pathogens from the body. However, in FcγR-mediated autoimmunity, macrophages are one of the primary orchestrators of the inflammatory response that is attributed to pathogenesis. A common denominator of autoimmune diseases, such as

rheumatoid arthritis (RA) and systemic lupus erythematosus (SLE), are autoantibodies that form immune complexes (ICs) with self-antigen [4, 5].

Using the FcγR to regulate the immune and inflammatory response

Antibody based immunotherapies that activate FcγRs are attractive agents for treating cancers to autoimmune diseases. While antibody therapy for cancer is meant to employ the immune system on a specific target, conversely, suppressing FcγRs activities for autoimmunity requires the opposite, competitive inhibitors that can bind and displace autoantibodies without initiating an immune response. Though opposite goals, successful drug design in either case requires a thorough understanding of the mechanisms governing FcγR activation and deactivation.

Rituximab is an anti-CD20 antibody used to treat many types of B-cell lymphomas and hyper-active B-cell rheumatological disorders. During intravenous delivery of Rituximab, B cells expressing the CD20 protein on their surface are decorated by the Rituximab antibody leading to their recognition by immune cells including macrophages and NK cells expressing FcγRs. Normal and malignant B cells are depleted predominantly by macrophages via antibody-dependent cell phagocytosis (ADCP), and secondarily by ADCC and complement mediated cell death [26, 27]. The addition of Rituximab to chemotherapy significantly enhances response to treatment [28]. Rituximab represents a shift in rheumatological and cancer treatments and is an example of the potential immunotherapies hold.

Rituximab is an example of directing an antibody based immune response via FcγRs. For IgG-mediated autoimmune diseases, FcγR inhibition is an attritive strategy to

inhibit IC-associated autoimmune diseases [29]. Autoimmune diseases such as RA in mouse models, and human autoimmune diseases such as acute immune thrombocytopenia purpura (ITP) and Kawasaki disease have been effectively treated using single IgG Fc fragments and IVIG [30-32]. However, using just the IgG fragments or IVIG is not ideal because large doses are required due to the 1-1 Fc-FcγR binding in order to displace polyvalent ICs. An alternative approach would be to design a therapeutic antibody with a higher avidity than the autoantibodies that could inhibit FcγR activation by blocking binding of autoantibody ICs. Doing so without accidentally activating receptors represents a challenge in the design of therapeutic antibodies. A strategy for designing a competitive FcγR inhibitor is to make a multivalent Fc molecule with a high affinity and avidity to displace the auto-polyvalent ICs.

One of the challenges facing the design of therapeutic antibodies is potential for accidentally causing receptor clustering and activating the FcγRs, causing further damage. Knowing the minimum number of receptors required to activate and propagate signal is key to developing therapeutics. Recently, this question was interrogated through the engineering of multivalent Fc molecules of varying sizes and geometries. The minimum requirement to activate FcγRs was an X-shaped pentameric molecule while a trimer was able to dock FcγRs with a high affinity and avidity without activating the receptor. The trimer showed promising results in animal models of RA and SLE and as a potent inhibitor [6].

While much of the signaling has been deciphered, the assembly of the FcγR activating cluster has yet to be sufficiently defined. In this dissertation, two aspects of FcγR activation will be addressed. The first addresses how the local topography and

actin regulators facilitate FcγR clustering at the phagocytic cup. Second, valency of the FcγR was interrogated using fluorescently labeled multivalent Fc molecules to understand the mechanistic differences in activation among varying cluster sizes. Together, this dissertation provides insights into FcγR activation that contributes to a basic understanding of immunology and may be informative for drug design strategy.

References

1. Li, X. and R.P. Kimberly, *Targeting the Fc receptor in autoimmune disease.* Expert Opin Ther Targets, 2014. **18**(3): p. 335-50.
2. Nimmerjahn, F. and J.V. Ravetch, *Fcγ receptors as regulators of immune responses.* Nature Reviews Immunology, 2008. **8**: p. 34.
3. Zhang, Y., A.D. Hoppe, and J.A. Swanson, *Coordination of Fc receptor signaling regulates cellular commitment to phagocytosis.* Proc Natl Acad Sci U S A, 2010. **107**(45): p. 19332-7.
4. Cojocaru, M., et al., *Manifestations of systemic lupus erythematosus.* Maedica, 2011. **6**(4): p. 330-336.
5. Schellekens, G.A., et al., *Citrulline is an essential constituent of antigenic determinants recognized by rheumatoid arthritis-specific autoantibodies.* The Journal of clinical investigation, 1998. **101**(1): p. 273-281.
6. Ortiz, D.F., et al., *Elucidating the interplay between IgG-Fc valency and FcγR activation for the design of immune complex inhibitors.* Science Translational Medicine, 2016. **8**(365): p. 365ra158.
7. Kuster, H., H. Thompson, and J.P. Kinet, *Characterization and expression of the gene for the human Fc receptor gamma subunit. Definition of a new gene family.* J Biol Chem, 1990. **265**(11): p. 6448-52.
8. Brandsma, A.M., et al., *Clarifying the Confusion between Cytokine and Fc Receptor "Common Gamma Chain".* Immunity, 2016. **45**(2): p. 225-6.
9. Call, M.E. and K.W. Wucherpfennig, *Common themes in the assembly and architecture of activating immune receptors.* Nat Rev Immunol, 2007. **7**(11): p. 841-50.
10. Blazquez-Moreno, A., et al., *Transmembrane features governing Fc receptor CD16A assembly with CD16A signaling adaptor molecules.* Proc Natl Acad Sci U S A, 2017. **114**(28): p. E5645-E5654.
11. Goodridge, H.S., et al., *Activation of the innate immune receptor Dectin-1 upon formation of a 'phagocytic synapse'.* Nature, 2011. **472**(7344): p. 471-5.
12. Lin, K.B., et al., *The rap GTPases regulate B cell morphology, immune-synapse formation, and signaling by particulate B cell receptor ligands.* Immunity, 2008. **28**(1): p. 75-87.
13. Batista, F.D., D. Iber, and M.S. Neuberger, *B cells acquire antigen from target cells after synapse formation.* Nature, 2001. **411**(6836): p. 489-494.
14. Grakoui, A., et al., *The Immunological Synapse: A Molecular Machine Controlling T Cell Activation.* Science, 1999. **285**(5425): p. 221.
15. Flannagan, R.S., V. Jaumouille, and S. Grinstein, *The cell biology of phagocytosis.* Annu Rev Pathol, 2012. **7**: p. 61-98.
16. Freeman, S.A., et al., *Integrins Form an Expanding Diffusional Barrier that Coordinates Phagocytosis.* Cell, 2016. **164**(1-2): p. 128-140.
17. Lowell, C.A., *Src-family and Syk kinases in activating and inhibitory pathways in innate immune cells: signaling cross talk.* Cold Spring Harb Perspect Biol, 2011. **3**(3).
18. Mocsai, A., J. Ruland, and V.L. Tybulewicz, *The SYK tyrosine kinase: a crucial player in diverse biological functions.* Nat Rev Immunol, 2010. **10**(6): p. 387-402.
19. Nimmerjahn, F. and J.V. Ravetch, *Fcgamma receptors: old friends and new family members.* Immunity, 2006. **24**(1): p. 19-28.
20. Schwartz, S.L., et al., *Differential mast cell outcomes are sensitive to FcepsilonRI-Syk binding kinetics.* Mol Biol Cell, 2017. **28**(23): p. 3397-3414.
21. Katz, Z.B., et al., *A cycle of Zap70 kinase activation and release from the TCR amplifies and disperses antigenic stimuli.* Nat Immunol, 2017. **18**(1): p. 86-95.

22. Murphy, K.W., Casey, *Janeway's Immunology*. Vol. 9. 2017, New York and London: Garland Science Taylor and Francis Group. 924.
23. Getahun, A. and J.C. Cambier, *Of ITIMs, ITAMs, and ITAMis: revisiting immunoglobulin Fc receptor signaling.* Immunol Rev, 2015. **268**(1): p. 66-73.
24. May, R.C. and L.M. Machesky, *Phagocytosis and the actin cytoskeleton.* Journal of Cell Science, 2001. **114**(6): p. 1061.
25. Mak, T.M.S., Mary E.; Jett, Bradley D., *Primer to The Immune Response*. Second ed. 2014 Elselvier, Academic Cell. 702.
26. VanDerMeid, K.R., et al., *Cellular Cytotoxicity of Next-Generation CD20 Monoclonal Antibodies.* Cancer Immunol Res, 2018. **6**(10): p. 1150-1160.
27. Gul, N. and M. van Egmond, *Antibody-Dependent Phagocytosis of Tumor Cells by Macrophages: A Potent Effector Mechanism of Monoclonal Antibody Therapy of Cancer.* Cancer Res, 2015. **75**(23): p. 5008-13.
28. Dotan, E., C. Aggarwal, and M.R. Smith, *Impact of Rituximab (Rituxan) on the Treatment of B-Cell Non-Hodgkin's Lymphoma.* P & T : a peer-reviewed journal for formulary management, 2010. **35**(3): p. 148-157.
29. Flaherty, M.M., et al., *Nonclinical evaluation of GMA161--an antihuman CD16 (FcgammaRIII) monoclonal antibody for treatment of autoimmune disorders in CD16 transgenic mice.* Toxicol Sci, 2012. **125**(1): p. 299-309.
30. Anthony, R.M., et al., *Recapitulation of IVIG Anti-Inflammatory Activity with a Recombinant IgG Fc.* Science, 2008. **320**(5874): p. 373-376.
31. Oates-Whitehead, R.M., et al., *Intravenous immunoglobulin for the treatment of Kawasaki disease in children.* Cochrane Database Syst Rev, 2003(4): p. CD004000.
32. Debré, M., et al., *Infusion of Fcγ fragments for treatment of children with acute immune thrombocytopenic purpura.* The Lancet, 1993. **342**(8877): p. 945-949.

CHAPTER II. ACTIN NUCLEATORS AND MEMBRANE BENDING SHAPE THE SIGNALING OF FCγ RECEPTOR-MEDIATED PHAGOCYTOSIS

Abstract

FcγR-mediated phagocytosis is initiated upon the clustering of FcγRs once they have bound IgG on the surface of a target. While the signaling machinery driving phagocytosis is well described, little is known about how nanoscale membrane topography facilitates receptor activation at the phagocytic synapse and its effect on tall transmembrane phosphatases. Here, we applied new methods capable of capturing membrane curvature using polarized Total Internal Reflection Fluorescence (polTIRF) microscopy to visualize the topography of the macrophage membrane during frustrated phagocytosis of mobile IgG on a supported lipid bilayer. The membrane curvature was examined for a small group of mutants dysfunctional in actin nucleators identified in a genetic screen for phagocytosis. Formation of the phagocytic cup involved robust organization of membrane topography and indicated that the force provided for lamellipodia advancement is formed by specific orientation of membrane and cytoskeleton. Specifically, the macrophage membrane remains flat against the target surface during phagocytosis and this region is followed by the $\alpha_M\beta_2$ integrin. Moreover, we demonstrate that the WAVE2 regulatory complex is essential for the formation of this topography and the lateral actin polymerization that provides the driving force for the leading-edge dynamics of the lamellipodia.

Introduction

Phagocytosis is responsible for debris and pathogen clearance. It is initiated in specialized phagocytes by a number of distinct receptors that can recognize innate signals or antibodies of an opsonized target [1, 2]. The FcγR is a potent promotor of phagocytosis in response to binding the Fc portion of target-associated Immunoglobulin G antibodies (IgG). Macrophages are professional phagocytes and express high levels of FcγR. Phagocytosis by macrophages depends on a balance of activating and inhibitory receptors that contain either immunotyrosine activation motifs (ITAMs) or immunotyrosine inhibition motifs (ITIMs), respectively. Receptor clustering (referred to as microclustering) allows for FcγRs to spatially exclude phosphatases and arrange ITAMs in close enough proximity for Syk kinase signal amplification [1, 3]. An aspect of FcγR clustering that is not completely understood is how the local topography facilitates the scaffolding of FcγRs, signaling molecules, and the cytoskeleton.

For successful signal amplification, the phagocytic cup or space between target and macrophage, called the immunological synapse (IS), must exclude the plentiful phosphatases on the macrophage surface. It has been shown that phosphatases CD45 and CD148 have large extracellular domains and can be excluded from the phagocytic cup during phagocytosis of glass beads [4]. In T and B cells, T and B cell receptors coalesce into a central signaling unit where phosphatases are physically squeezed out by the tight space created at the IS [5-7]. More recently, a similar clustering phenomenon was observed in the FcγR upon engagement with IgG on a mobile supported lipid bilayer [8]. In the case of the FcγR, Syk kinase was recruited to FcγR microclusters driving

production of freely diffusing Phosphatidylinositol (3,4,5)-trisphosphate ($PI(3,4,5)P_3$) and polymerization of lamellar actin followed by retrograde flow [8].

In the context of a rigid target surface, akin to bacterial and fungal cell walls, the signaling of the FcγR is amplified through the help of integrin. Rather than a tight IS being sufficient to spatially exclude phosphatases, integrins created a diffusional barrier between phosphatases and FcγR clusters and were shown to lower the threshold for required opsonin to complete phagocytosis[3]. Integrin recruitment to FcγR-mediated phagosomes has been observed, where the indicators of integrin activation, vinculin and talin, were found at phagocytic cups forming around IgG coated beads [9, 10]. The complement receptor 3 (CR3), referred to as $\alpha_M\beta_2$ integrin or CD11b/CD18 , is recruited to FcγR phagosomes in addition to being able to mediate phagocytosis by itself when engaged by the complement component C3b [11]. $\alpha_M\beta_2$ however, is one of the most promiscuous integrins and binds a variety of ligands that can be found on target cells, such as carbohydrates and components of the extracellular matrix: fibronectin, fibrinogen, and collagens [12]. Its promiscuity makes it a prime candidate for a secondary receptor in low antigen density, as it lowers the threshold for required opsonin [11]. In addition to forming a diffusional barrier and being a co-receptor, integrins have been found to form a dynamic podosome-like structure at the base of the phagocytic cup. That is believed to enable the tight contact between phagocyte and the phagocytic target as well as create a physical barrier. This allows kinase signal amplification and enables the progressive engagement of FcγRs while giving a point of a support to the lamellipodia [11].

As current literature suggests, integrins are attractive candidates for mechanistically explaining anchoring of the actin cytoskeleton at the phagocytic cup. To date, no mechanisms have been provided that link the FcγR to the actin cytoskeleton, thus it remains unclear as to how actin polymerization provides the force necessary for phagocytosis. Thus far, the players in actin nucleation that have been studied in this context have predominantly been vinculin, talin, and Arp2/3. Arp 2/3 nucleates and branches actin to form actin networks during lamellipodia protrusions. In *Arp2c*$^{-/-}$ (actin-related protein 2/3 subunit 2) macrophages, where formation of the Arp2/3 complex was compromised, FcR-mediated phagocytosis was not disrupted, while integrin dependent functions, such as complement-mediated phagocytosis were [13]. However, in a phagocytic screen, vinculin, talin, and all integrins were found to be dispensable, while gene knockouts for Arp2/3, *Actr2* and *Actr3* (actin-related protein 2 and 3), had mixed results of its necessity. The WAVE2 complex was found to be required for phagocytosis, while knockout of WASP enhanced phagocytosis.

The Wiscott Aldrich Syndrome Protein (WASP) family is a family of actin regulators that are understood to be responsible for regulating the dynamics of the actin cytoskeleton. They are responsible for the stimulating steps for Arp2/3 actin nucleation through its conserved C-terminal VCA (Verprolin-homology, Central, Acidic) [14, 15]. The WASP family verprolin homologous protein (WAVE) plays a role in processes such as cell adhesion, cell division, and migration, among others [15]. In T cells, WASP was found to generate dynamic F-actin foci at the T cell receptor's (TCR) IS. Though not required for actin polymerization at the IS, the dynamic architecture made via WASP

amplified the downstream signals that are required for optimum immune response, including the PLCγ1 activation pathway [16].

The WAVE regulatory complex (WRC or referred to simply as WAVE) is a heteropentameric complex made up of two subcomplexes; the first being a dimer of Cyfip1 (Sra1) and Nap1 (also known as Hem-1 or Nckap1l) and the second being a trimer made up of the N terminus of WAVE, Abi1, and Brk1 (also called Brick1 and HSPC300)[14, 17]. Cyfip1 links Nckap1l to activated Rac, suggesting that Rac may regulate WRC activation through Nckap1l and Cyfip1 [17].

Within the WAVE complex, three possible isoforms of the WAVE protein occur: WAVE1, WAVE2, and WAVE3. WAVE1 and WAVE3 are expressed mostly in neuronal cells. WAVE2 is expressed ubiquitously, but is the only WAVE protein expressed in hematopoietic stem cells and highly expressed in leukocytes [18-20]. WAVE's major role is Arp2/3 activation during protrusions of the plasma membrane and cell motility. WAVE2 (the WAVE complex containing the WAVE2 isoform), specifically, is associated with peripheral membrane ruffling, cell mobility, and lamellipodia formation [14]. Hem-1, or Nckap1l, are specific to hematopoietic cells. Immunoprecipitation of Hem-1of human promyelocytic leukemia cells, established that Hem-1 associates with WRC proteins WAVE2, Abi1 and Cyfip1/2 [21]. Hem-1 is thought to organize the leading edge lamellipodial formation by controlling a Rac/F-actin-mediated feedback loop [21]. This was further supported via TIRF microcopy, where Hem-1 waves were correlated with the spread of the advancing leading edge. These waves of Hem-1 are thought to stimulate nucleation of actin at the leading edge

and may be vital for phagocytosis[21]. Additionally, work done in *Hem1*$^{-/-}$ neutrophils, exhibit major defect in phagocytosis [21].

While it is established that the formation of an IS involves exclusion of phosphatases and dynamic actin polymerization, the role of the local topography has not been explored. We predict that the plasma membrane must be dynamic in order to facilitate the diffusion and scaffolding of receptors, adhesion proteins, and other accessory proteins necessary for phagocytosis. Our lab developed a unique method to measure membrane bending dynamics. This method, polarized total internal fluorescence microscopy (polTIRF), uses the orientation of the dipole of a lipophilic dye, DiI, under selective polarized excitation in either vertical or horizontal membrane to capture the dynamics of membrane curvature in living cells [22]. Here, we applied this method to interrogate changes in membrane topography during formation of the phagocytic lamellipodia in the context of frustrated phagocytosis on a mobile surface. We found that in the context of the mobile antigen, the phagocytic cup forms an IS at the leading edge of an advancing lamellipodia that has an overall flat membrane which we predict would squeeze out phosphatases such as CD45. Additionally, immunofluorescence revealed integrin α_M anchors the actin cytoskeleton behind a leading row of FcRs. These findings provide a potential explanation for a target-seeking force that pushes the membrane of the phagocytic cup into close juxtaposition with the target and may exclude large extracellular domain containing proteins such as CD45.

Through CRISPR gene disruptions of the components of the WASP, WAVE (WRC), and Arp2/3 complexes, we have demonstrated that the actin nucleators are possibly specific to directionality of actin polymerization. Knockouts for *Wasf2*

(WAVE2) and *Nkap1l* of the wave complex and *Actr2* of the Arp2/3 complex, dramatically altered the organization of the leading-edge and the distribution of FcγR, suggesting that the WAVE complex is required for actin polymerization in lateral lamellipodia protrusions. These findings provide further insight into the local environment facilitating FcγR cluster assembly and signaling.

Results

Measuring Membrane Bending During Frustrated Phagocytosis

Supported lipid bilayers on glass, containing biotinylated POPC, were used as a flat, mobile, target to image the organization of FcγRs and the morphology of the pseudopod in TIRF. Fluorescently labeled anti-biotin IgG2a was used to opsonize the bilayer and fetal liver macrophages (FLMs) were dropped on the bilayers (Fig. 2.1A). FcγR engagement with the surface-associated IgG2a results in a potent frustrated phagocytic response; in which the cell attempts to engulf the surface but cannot due to its size. Fluorescent IgG2a allowed for visualization of FcγR clustering and their movements at the macrophage-target interface. In WT cells, clusters formed during the forward movement of the lamellipodia (Fig.2.1B) and then detached from the leading edge and trafficked back in towards the center of the phagocytic cup (Fig. 2.1C). Figure 2.1A shows a representation (not to scale) of an FLM engaging via its FcγRs with the opsonized bilayer. Figure 2.1D shows an example of a macrophage over a timelapse, whose FcγRs engage the IgG2a and respond by expanding outward as it attempts to engulf the bilayer. As it does so, receptors were pulled toward the center of the cell. This was studied in mouse fetal liver macrophages (FLM) (top), but human PBMC macrophages (bottom) were shown to behave in the same way as mouse macrophages.

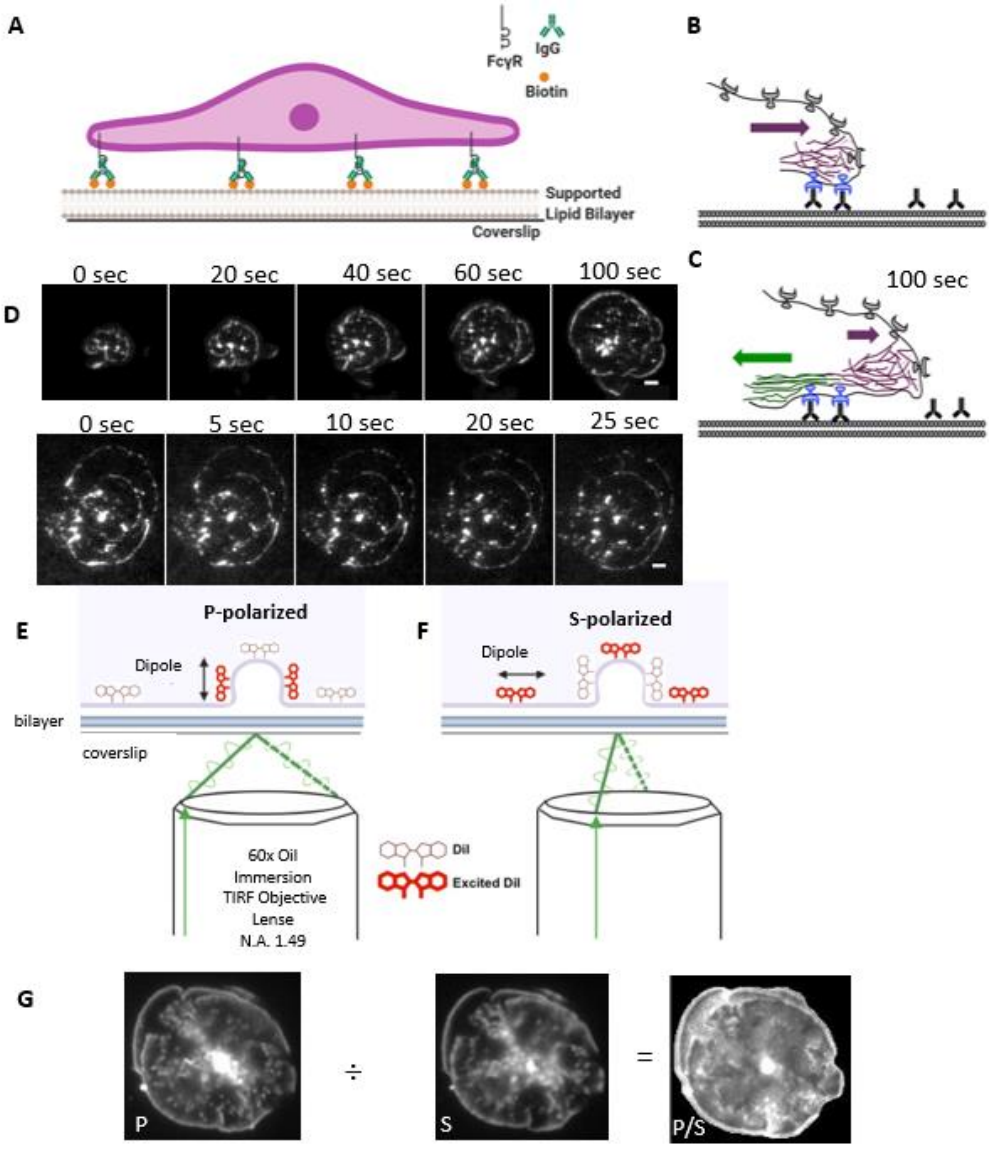

Figure 2.1 PolTIRF imaging of membrane bending and FcγR organization during engagement of mobile IgG. A) Frustrated phagocytosis was done using mobile supported lipid bilayers (SLB) containing biotin-PE lipids that were opsonized with fluorescent antibodies (Created with BioRender). B-C) A representation of the leading edge was adapted from [8] and shows the leading edge advancing out radially, which required actin polymerization (purple) (B) that presumably propelled active FcγRs forward (C) until a process similar to retrograde actin flow (green) caused FcγRs to retract toward the center of the cell (C) [8]. D-E) Response to the IgG opsonized SLB was similar between mouse fetal liver macrophage (FLM) (top) and human PBMCs (bottom). Scale bare represents 2um. E-F) polTIRF utilizes directionally polarized light to excite a lipophilic dye, DiI [22]. DiI's dipole aligns parallel to the bilayer, allowing detection of vertical membrane with p-polarized light (E) or horizontally membrane with s-polarized light (F). G) The polTIRF is used to image vertical membrane (P image) and horizontal membrane (S image). These images are divided to create a P/S ratio image to show curvature, where the areas of highest intensity refer to more curvature and the low intensity refers to less curvature.

For curvature measurements, images of DiI labeled macrophages were used to calculate total curvature. When DiI is vertical, the dipole is vertical and is excited by vertically, or p-polarized light. Likewise, the horizontally oriented DiI is excited by horizontally, or S-polarized light. Figure 2.1E and 2.1F represents the 2-point TIRF setup with the laser beam bouncing off the glass-water interface with either p-polarized light (E), or S-polarized light (F). The cartoon demonstrates the selective excitation of DiI during endocytosis were the vertically oriented DiI fluoresces when excited by p-polarized light (F) and horizontally oriented DiI fluoresces when excited with S-polarized light (E). Figure 2.1G is an example of polTIRF using P and S-polarized light to of primarily vertical and horizontal membrane respectively. The P/S ratio images were made by dividing the P-image by the S-image to yield an image of total curvature.

Membrane is most vertical near advancing edge and initial contact point

Timelapse imaging revealed that membrane curvature is highest at the leading edge and then flattens as contacts with the target are established. Figure 2.2A shows a representative montage of timelapse images of the IgG2a AF488, P/S ratio, and the resulting merged images of the two. Close examination and a line scan of the leading edge showed vertical membrane followed by a flat region behind the zone of IgG2a clusters, interspersed with occasional spots of high curvature (Fig. 2.2B-C). Line scans from the center of the cell to the most outward edge showed that clusters of IgG2a were found in regions of less vertical membrane (Fig. 2.2D-F). The membrane immediately behind clustered receptors has a lower P/S ratio, which suggests that as contacts with the target are made, and the macrophage's pseudopod advance outward, the membrane remains flat against the target. These data demonstrate highly organized clusters and

membrane topography that orchestrate the phagocytic process. The progression of the leading edges suggests that contact is established in the center of the cell and there is a force pushing out laterally.

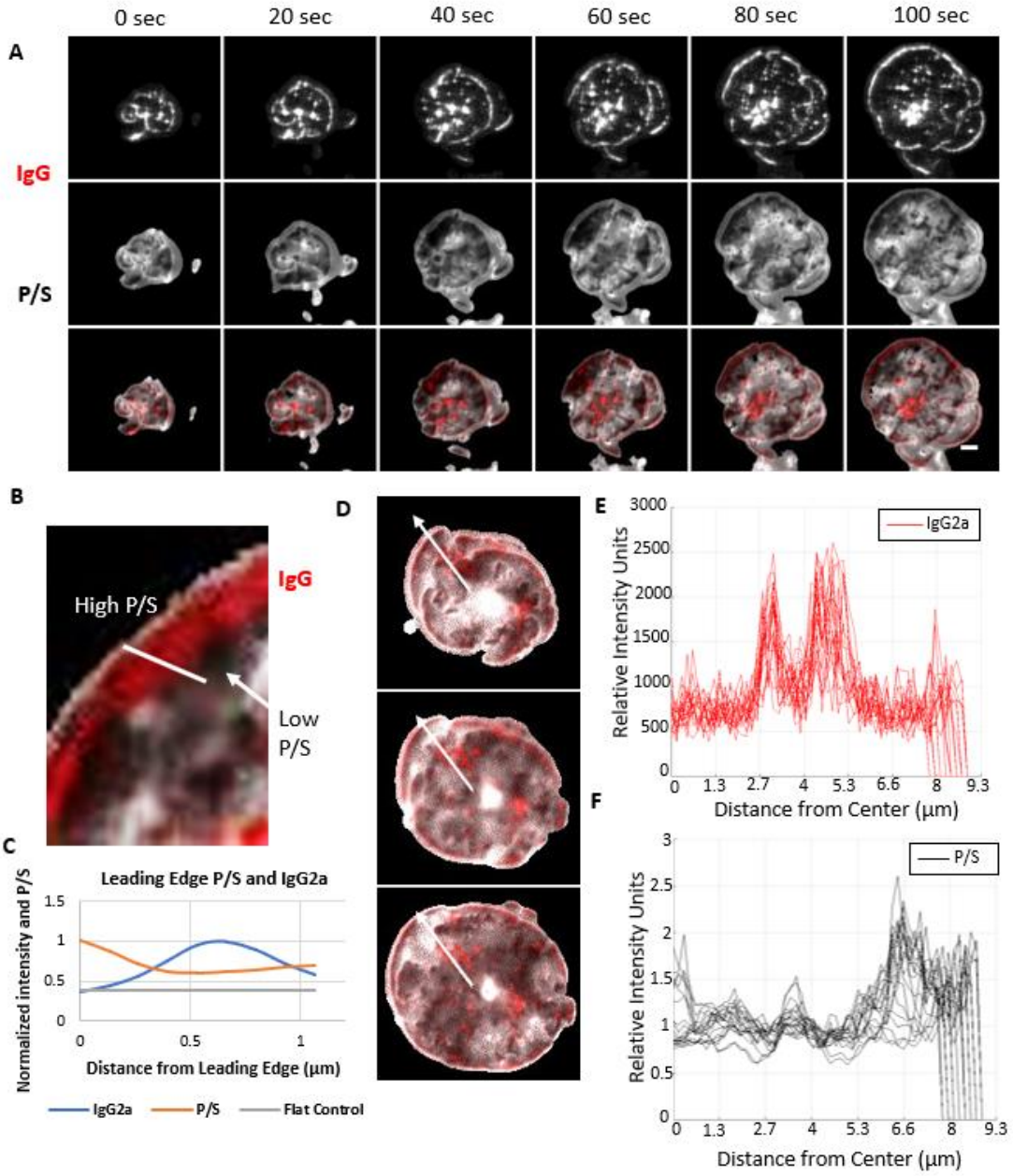

Figure 2.2 PolTIRF analysis of membrane topography relative to sites of FcγR engagement. A) Timelapse imaging of IgG and P/S signals during frustrated phagocytosis showed that the membrane behind the IgG leading edge was flat and the highest curvature remained further inward, toward the center of the cell (Scale bar=2um). B) A close-up of the leading edge of the cell shows the very front of the cell is curved, followed by mostly flat membrane that sharply curve in some areas. C) A line scan of a single frame at the leading edge verifies that the front of the pseudopod is vertical and then flattens out where IgG2a engages with FcγRs, but it still more curved than the flat control (DiI labeled SLB). D) Line scans across the cell's radius for a 20 frame timelapse are represented as an arrow across three of the twenty frames measured. E-F) These line scans (not the same cell from panel A) of the IgG2a (E) and P/S (F) show peaks of IgG2a where clusters presumably retract towards the center and at the leading edge. While curvature is dynamic, overall P/S ratio remains relatively low other than near the leading edge.

Cytoskeleton at the phagocytic cup is dependent on actin and adaptors

Membrane curvature and the frustrated phagocytosis assay demonstrated high organization of the membrane and receptor clusters that prompted interrogation of the players that facilitate such organization. Clustered FcγRs recruit Syk which drives production of diffusing $PI(3,4,5)P_3$, which in turn, coordinates lamellar actin polymerization [8]. The dependence of macrophages on actin polymerization for the formation of pseudopodia in our supported lipid bilayer system, was validated by treating macrophages with latrunculin before dropping them on the opsonized bilayers. Latrunculin is a toxin made by the sponge, *Latrunculia genus*, that prevents actin polymerization by binding actin monomers. Latrunculin treated cells were able to make contact and were able to spread a limited distance but exhibited poor organization of receptor clusters and failed to form a discrete leading edge (Fig. 2.3A). We observed that the curvature of the plasma membrane (P/S ratio) remained flat in the region of contact and shows little to no change over the course of timelapse imaging, indicating that the higher degree of organization observed in between untreated macrophages required additional actin polymerization. Latrunculin appeared to prevent full spreading on the bilayer. Macrophages were able to spread, but not to the same extent as untreated macrophages. Additionally, the FcγR clusters were unable to organize the same way and remained in disorganized patches. This suggests a lack of lateral actin polymerization. Rather, it appears cells contacted the bilayer, clustered receptors where the macrophage surface made contact, but could not extend much laterally to advance the leading edge and engage more antibody. While actin is clearly important for the advancing leading

edge and overall organization of the phagocytic cup, it is not known to be physically connected to the FcγR, suggesting an important role of actin regulators.

We next wanted to determine other molecules responsible for actin coordination during phagocytosis. We first looked at integrins, as they are adhesion proteins known to anchor the actin cytoskeleton, and they are known to be a diffusional barrier during frustrated phagocytosis to prevent large phosphatases, such as CD45, from dephosphorylating activated receptors [3]. Knowing this, immunofluorescence was applied to the supported lipid bilayer system, which required gentle washes that left a small volume in the Leiden chamber, to prevent disruption of the bilayer. Figure 2.3B represents the process of immunofluorescence on a supported lipid bilayer. Integrins expressed in FLMs, β_1, β_5, and α_M were stained. α_M was the only one of the integrins that was associated with microclusters. This is demonstrated in Figure 2.3C whereas β_1 and β_5 show no correlation with clustered IgG2a, but α_M localizes to the flat regions (P/S, Fig. 2.3C) behind the IgG2a. Next, we applied the same system to label actin with phalloidin. Figure 2.3D again shows a localization of actin that closely mimics the localization of both α_M and low P/S ratio membrane. These data suggest that the actin cytoskeleton facilitates a tight synapse between the target and phagocytic cup, creating a flat membrane topography, and is anchored by α_M. This topography may also facilitate the scaffolding of other accessory proteins that are necessary for phagocytosis.

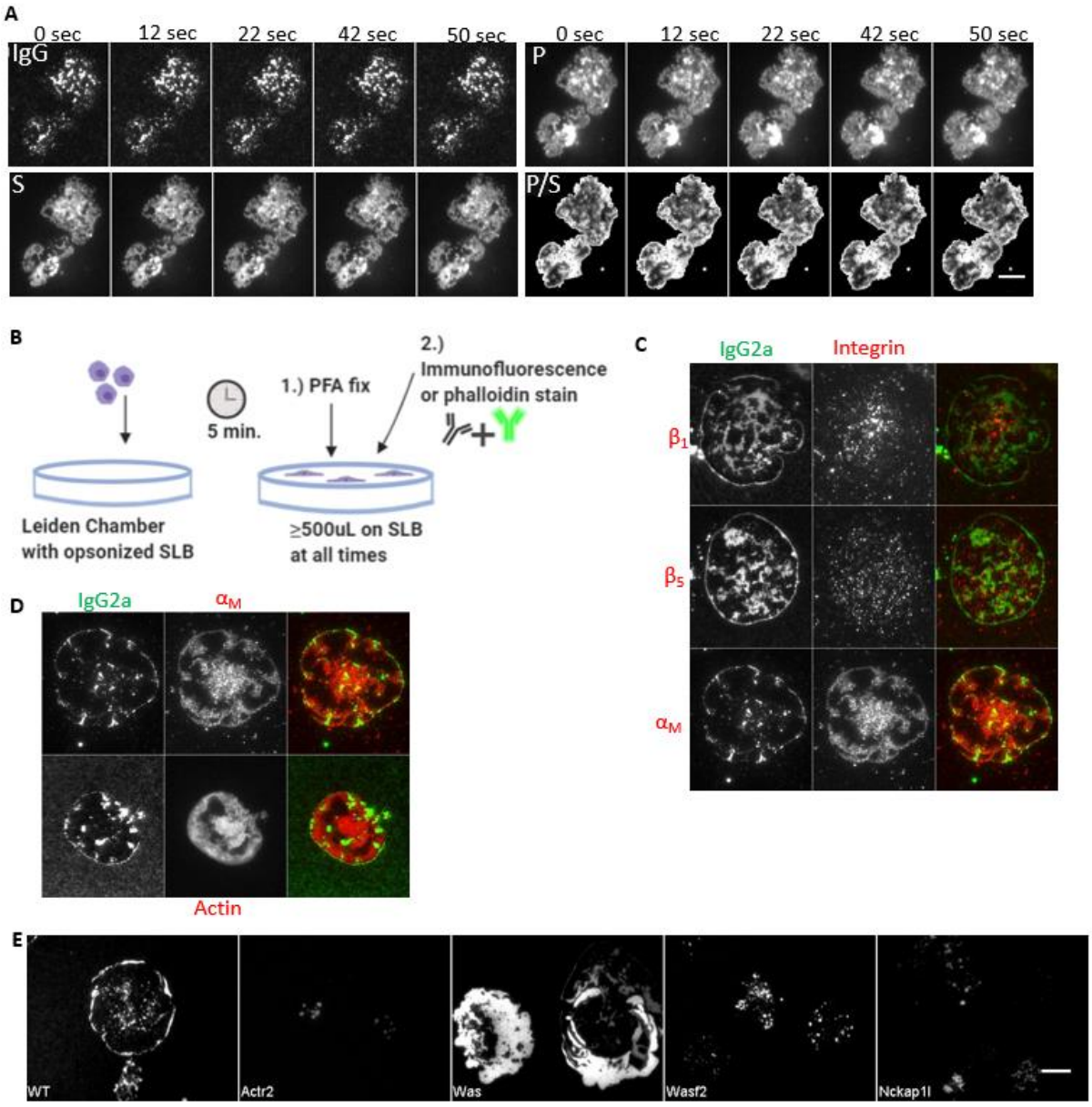

Figure 2.3 Actin, actin adaptors, and integrins shape the topography at the phagocytic cup. A) Latrunculin treated FLM cells show lack of organization of FcγR clusters during frustrated phagocytosis of a mobile target. Curvature is relatively flat and spreading of the cell is minimal. B) Immunofluorescence of FLM cells shortly after being dropped on the IgG opsonized bilayer allows staining of actin and integrins. C) Immunofluorescence of integrins expressed in FLM cells shows α_M as candidate for actin cytoskeleton anchoring. D) Comparing staining of α_M with actin (phalloidin), the pattern of localization is very similar and coincide with the area of flat membrane behind the leading edge of the phagocytic cup. E) Actin adaptors required for phagocytosis: Snapshots of gene knockouts of *Actr2*, *Wasf2*, and *Nckap1l* show an inability to expand laterally but could form microclusters (namely in *Wasf2* and *Nckap1l*). While *Was* knockouts experienced hyper engagement lateral spread but poorly organized microclusters. Scale bars represent 5um.

These results indicated that while α_M appears to be in a location consistent with anchoring the cytoskeleton to the plasma membrane for actin polymerization. Meanwhile, results of a whole genome screen conducted in the Hoppe lab indicated that that α_M was not necessary for phagocytosis (data not shown). Rather, macrophages were able to internalize IgG coated particles without α_M or β_2 and still establish a connection to the cytoskeleton. In addition, the screen showed other proteins, namely actin adaptors and regulators of the WAVE and Arp2/3 complexes, that were required for phagocytosis. To evaluate the structure of the phagosome/target contact, we applied TIRF microscopy of gene-disrupted macrophages. On the IgG2a opsonized bilayer, the actin nucleator *Actr2* knockouts only made punctate attachments to the bilayer, with no expansion from the central point of contact (Fig. 2.3E). The *Was* mutants (coding for WASP) were able to form an advancing pseudopod, however, the structure of the contact was dramatically altered, resulting in large regions in contact with the target surface. This leads us to believe that this protein may be important for integrin activation and organization of contact sites. Thus, *Was* mutants failed to elevate plasma membrane above the target membrane, but rather simply just flatten out membrane across it. The WAVE complex proteins, *Wasf2* and *Nckap1l*, both established contact with the opsonized surface but failed to organize a lamellipodia leading edge as in the parental examples. The effect of *Nckap1l* was even more debilitating than *Wasf2*. These data suggest WASP is not required for the advancing leading edge but may be involved in integrin activation, that props the cell up and for activating Arp2/3 nucleation at the immediate contact area. Alternatively, these data may also further confirm WASP's involvement in regulation of Arp2/3 at the podosome or even suggest a role as a negative regulator of the FcγR. The

WAVE complex appears to be vital for activating Arp2/3 to provide lateral actin branching at the leading edge. Nckap1l, the link between WAVE2 and Cyfip1, which binds to Rac, may be part of the regulation of the WAVE-mediated activation of Arp2/3. Without it, it is unable to activate the Arp2/3 and inhibits the cells to laterally nucleate new actin or branch existing actin.

Discussion

In the context of therapeutic antibodies, the antigen, IgG and the FcγRs are mobile at the macrophage target interface. Our work focuses on addressing how the topology of the membrane organizes FcγR dependent phagocytosis. This is in contrast to previous work on phagocytosis that has been studied in the context of immobile antigen. Studying in the context of mobile antigen provides insight into phagocytic response of immunotherapies.

Understanding that phagocytosis is dependent on the exclusion of phosphatase from clustered FcγR-IgG synapse, we predicted that the FcγR clustering behavior was associated with deformation of the plasma membrane to spatially exclude phosphatases. We expected a flat region where the receptor: antibody complexes would form a tight space at the IS and a sharp vertical membrane transition at sites where tall phosphatases, extending approximately 30nm from the cell surface, would force the macrophage membrane to bend and make room for it against the target. Indeed, our polTIRF imaging demonstrated that IgG-rich regions of contact corresponded to low P/S (flat) regions of membrane that were enveloped by regions of vertical membrane, suggesting that molecular heights influenced the membrane topography at the contact site. This finding is consistent with IgG-FcγR complexes extending into the extracellular space about 6nm

and that the SLB lays on flat glass. Most vertical membrane existed at the very central point of contact of the cell and at the leading edge which suggests that taller molecules may create a separation between macrophage membrane and the coverglass. We can predict that the vertical nature of the leading edge was from the flow of PM that occurs as antibody meets receptors, as is suggested by the zipper model. Additionally, polymerizing actin at the leading edge may cause higher membrane bending due to local membrane tension pulling against the non-adherent side of the lamella.

Knowing that integrins were shown to serve as physical barriers between FcγRs and CD45 in the case of immobile antigen [3] and that the integrins involved in the complement receptor, $\alpha_M\beta_2$ are present at the phagocytic cup [23], we interrogated the involvement of integrins in the context of mobile antigen. To do so, the most highly expressed integrins in FLMs were immunostained (Fig. 2.3B) and α_M integrin, was associated with plasma membrane regions adjacent to or following advancing receptor microclusters at the leading edge, forming a ring (Fig. 2.3C). Additionally, phalloidin labeling of actin showed a similar localization of a ring around the cell, lying just behind the leading edge of the macrophage. These similarities imply that $\alpha_M\beta_2$ is responsible for anchoring the cytoskeleton at the phagocytic cup. It is possible that its function is twofold in allowing a close contact to be formed to spatially exclude phosphatases as well as act as a diffusional barrier in the few areas that may allow diffusion of the tall proteins. These observations reinforce that a podosome-like structures form at the base of the phagocytic cup.

Complement receptor, $\alpha_M\beta_2$ is present at the phagocytic cup [23] and activated integrins diffuse to activating FcγR and determine the efficacy of phagocytic response by

lowering the opsonin threshold needed for engulfment [3]. While in some cases, integrins appear to enhance the phagocytic response, our unpublished results indicate that $\alpha_M\beta_2$ was not required for phagocytosis. Rather, the Arp2/3 and WAVE2 machinery (*Actr2, Wasf2,* and *Nkap1l)* were necessary for organization of receptor clusters at the phagocytic cup and efficient phagocytosis. It is not yet clear if Arp2/3 and WAVE2 are necessary for actin dynamics and architecture or if they are involved in regulating other signaling processes.

Importantly, WASP, demonstrated through the *Was* knockout, was required for FcγR organization and we speculate that this was in-turn important for integrin activation and regulation of regulating the number of engaged FcγRs. It has been proposed that CalDAG-GEF1 serves as an adapter for integrins at FcγR clusters, as CalDAG-GEF1-null mice did not form integrin barriers for CD45 phosphatases[3]. This may be the case, at least in immobile antigen, but our TIRF data of the *Was* knockout suggests that the WASP complex may be involved in inside-out integrin activation to employ the kickstand structure to lift the cell off the target surface enough. Based on literature, this likely occurs at dynamic podosomes that form during target engulfment. Podosomes form upon the engagement of the extracellular matrix by integrins. At the core of podosomes, integrin β_1 is preferentially found, along with WASP [24, 25]. While β_1 is associated with WASP activation at the core, there is also evidence that WASP regulates integrin clustering at the initiation of podosomes. Specifically, in dendritic cells, WASP was associated with β_2 recruitment, but this recruitment did not occur in the absence of WASP and the concentric rings of integrins failed to form [26]. Drawing from literature and our data, it appears that WASP is associated with podosome initiation steps that

recruit and activate integrins, allowing podosome formation and the 'propping up' of the cell as was previously described.

If WASP indeed is associated with integrin recruitment and activation at the podosome, it appears that a lack of integrin activation still allows, and enhances, receptor engagement and clustering, demonstrated in the TIRF data. This result coincides with the enhanced eating from the phagocytic screen in the *Was* knockout bone marrow macrophages. Future work will look at membrane curvature in *Was* knockout cells, with the prediction that the membrane would be even flatter, with fewer dynamics and spikes in vertical membrane.

These data, in conjunction with literature showing the formation of dynamic podosomes [11] at the phagocytic cup, help shape a clearer picture of the phagocytic cup, It seems that WASP is associated with Arp 2/3 actin nucleation during podosome formation as well as with the initial recruitment and inside out activation of integrins that allow them to prop the cell up. Previously, it was suggested that receptor cross-talk between FcγRs and integrins [3] was responsible for the inside-out activation during frustrated phagocytosis, but these data suggest WASP has a significant role. In its absence, phagocytosis is still successful, but the synapse between target and phagocyte appears to be non-existent and receptor-IgG binding is enhanced. Despite an absence of organized receptor microclusters, the leading edge is still able to organize, unless the components of the WAVE complex are absent. In the case of *Wasf2* (WAVE 2) and *Nckap1l* knockouts, the cell was unable to organize its leading edge and advance it, despite appearing to form microclusters. This suggests the WAVE's role for stimulating actin nucleation may be directionally distinct from WASP; where the WAVE2 complex

is needed for the lateral Arp2/3 stimulation so that the pseudopod can advance around the target. WASP's stimulation for Arp2/3 may be specific to forward actin assembly as in the formation of dynamic podosomes (Fig. 2.4).

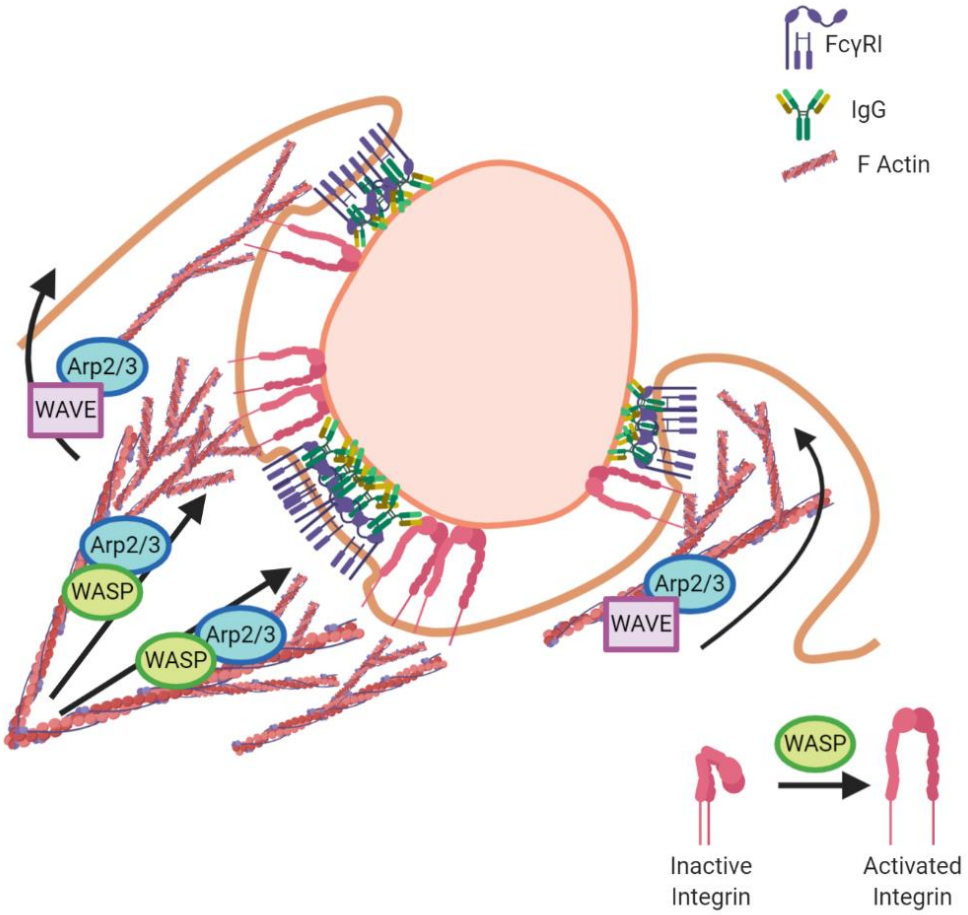

Figure 2.4 Actin Nucleators are specific to direction of membrane deformation. WASP stimulates Arp2/3 at dynamic podosomes and is associated with inside-out signaling necessary for activating integrin to prop cell up off the target surface. Meanwhile, Wave stimulates Arp2/3 to nucleate actin filaments for peripheral actin organization and lamellipodia formation. The short distance between receptor and antibody complexes at the IS create the flattest region of membrane while the height of integrins elevates the membrane. This makes a bend in the membrane and then facilitates a flat sheet of membrane associated with wrapping the pseudopod around the target. (Created with BioRender)

Phagocytosis requires FcγR clustering to propagate the intricate web of signaling the allows for engulfment of a target. This clustering has been shown in other receptors, such as the T cell receptor, to allow for a tight synapse to crowd out tall phosphatases. In macrophages, integrins were thought to not only be a valuable coreceptor, but also a physical barrier between phosphatases and clustered receptors FcγR [3]. We have demonstrated that much of the plasma membrane during frustrated phagocytosis is flat and that integrins appear to form a barrier behind the leading edge, suggesting that the phosphatase exclusion may be due to a combination of size exclusion and physical barriers. Additionally, we predict that WASP activates integrins through an inside-out activation, while WAVE2 is required for the lateral actin polymerization and successful engulfment of a target. These findings help shape a clearer understanding of FcγR-mediated phagocytosis and the local environment that facilitates signaling.

Methods

Supported Lipid Bilayer Formation

Supported lipid bilayers were formed by spontaneous fusion of lipid vesicles. For the opsonized bilayers, DSPE-PEG(2000) Biotin (Avanti Polar Lipids 880129) and POPC (850457 Avanti Polar Lipids) were mixed at a molar ratio of 1:100 with total lipid concentration of 500uM. The lipid mixture was then dissolved in chloroform and dried using a vacuum centrifugation to remove the chloroform, where the first minute ran at 30C and the remaining temperature was set to room temp. The lipid film was re-suspended in dPBS by initially vortexing and then sonicating for 5 minutes using a bath sonicator and then extruded through (Avanti Polar Lipids 610000) 100nm filter at least 13 times (Whatman Nucleopore Track-Etch 100nm membrane).

To form bilayers, liposomes were diluted by using 75uL liposomes for every 450uL of 2mM Mg^{2+} PBS. The dilution was then pipetted on the coverslip. The bilayer was formed on Piranha acid (H_2SO_4 (30 %, *v/v*):H_2O_2 (3:1, *v/v*)) cleaned coverslip and then dunked in water at about 42C to remove excess liposomes. The water was exchanged with dPBS followed by Hank's balanced Salt Solution for either imaging or opsonization (Corning). The bilayer coated coverslip was kept in a buffer solution during washing and transferring to imaging chamber to protect SLB from drying out and to keep it uniform. Either Alexa Fluor (AF) 647 (gene knockouts), 488 or Dylight (DL) NHS ester (ThermoFisher Invitrogen) was conjugated to anti-Biotin IgG (clone 3E6) for antibody fluorescent labeling. The antibody fluorophore varied by experiment to accommodate the other fluorophores being used in the experiments. The labeled

antibody was incubated with the 0.1% PEG-biotin SLB at 37 °C for 30 min. Excess IgG was washed with imaging buffer.

Data taken of knockouts was done on bilayers formed in 96 well glass bottom plates (Dot Scientific MGB096-1-2-LG-L). Plates were cleaned for bilayer formation using Hellmanex III Special Cleaning Concentration for cuvettes (Z805939 Sigma-Aldrich) by diluting the concentrated solution to a 2% solution in DI water and heating water between 30-37C in the microwave. Prepared Hellmanex was added in volumes of 150uL to each well of the 96 well plate and remained on a slide warmer set at 32C for 30 minutes. After the 30 minutes, the plate was rinsed thoroughly with DI water, undergoing at least 5 rinses. The liposomes were diluted similarly, using 12.5uL liposomes for every 150uL of 2mM Mg^{2+} PBS.

DiI labeling Cells in Suspension

Cells were removed from the dish using cold dPBS and then were spun down at 1500g for 5 minutes. Cells were resuspended and DiI (D282 ThermoFisher) labeled by resuspending the pellet in 500uL HBSS with 1ug of DiI stock (1mg/mL in DMSO). Cells were then spun down at 800 g for 3 minutes in the microcentrifuge and resuspended in HBSS and

Image Processing

Fiducial data collection and image registration. Single images were registered using calibration images acquired simultaneously on each of the four EMCCD detectors. A single image of 200 nm green beads (Life Technologies, Carlsbad, CA) immobilized

on a glass coverslip were excited using 445 nm excitation. Coordinates for registration were determined using the MATLAB (The MathWorks, Inc., Natick MA) *cpselect tool*. A rigid affine transformation was used to transform all points onto the red channel.

Line Scan Analysis

A customized MATLAB script utilizing the *improfile* function was used to generate line scans of the represented cell. A line scan was applied to the timelapse images and Figure 2D are the plotted line scans. Each line is the line scan for each frame. A binary mask was applied to the images line scans, resulting in a sudden drop to zero for frames that prior to the final frame. This is represented in the montage of Figure 2C where the line scan extends past the leading edge.

Cell Fixation and Staining

Five minutes after FLM cells were dropped on the bilayer they were fixed with 4% PFA for 20 minutes (exchanged HBSS 5x with PFA to make sure chamber was between 2 and 4% PFA).

Integrin staining: Cells were permeabilized for 20 minutes with 0.05% saponin. (washed 5x with dPBS) for integrin staining and then washed 5x with dPBS and then blocked with 0.001% BSA for 30 minutes (again 5x exchange was done). Samples were incubated overnight with appropriate antibody in 0.001% BSA at 4C. Integrin B1 (550531 BD Biosciences)-1:500 dilution; Integrin α_M-AF488 conjugated (CD11B) (557672 BD Biosciences) 1:200 dilution; Integrin B5 (ab15459 Abcam)- 1:500 dilution. Samples were washed 5x with dPBS the next day. The secondary antibody for integrin

B1, anti-Rat DL594 (SA5-10020 ThermoFisher), and B5, anti-Rabbit DL 594 (35560 Thermo Scientific Pierce Antibodies), were incubated at room temperature for one hour. Cells were washed 5 times and imaged with dPBS.

Staining actin with phalloidin

Actin was stained using a cocktail of 30 µL of phalloidin AF594 (A12381 Life Technologies), 0.1% saponin to 495µL of PBS + 0.001% BSA. For a final volume of 0.6mL. This is a 2x solution so that adding it to a chamber with about 500-600µL will have the final desired concentration of phalloidin and saponin. Solution was added to chamber and incubated at room temp 20 minutes.

The fixed samples underwent a final wash with dPBS 5 times and imaged in dPBS. Imaging was done using 50% 594nm laser for the phalloidin AF594 and 42% 488nm laser for AF488 IgG2a. Gain on the green camera was altered depending on the cell. No gain was necessary for the red channel.

Latrunculin

FLM cells were treated with 10uM Latrunculin B (428020 Millipore Sigma) for 30 minutes by adding 8uL of 2.5mM in DMSO to 2mL of the bone marrow media in a 6-well dish. Cells were removed from the dish at the end of the 30 minutes using cold dPBS and then were spun down at 1500g for 5 minutes. Cells were DiI labeled by resuspending the pellet in 500uL HBSS with 1ug of DiI stock, as previously described. Cells were then spun down at 800 g for 3 minutes in the microcentrifuge and resuspended in HBSS and imaged, looking at the IgG2a as well as the P and S channels.

Gene Knockouts (Conducted by Jason Kerkvliet)

Bone marrow was isolated from the femurs of B6J.129(Cg)-Gt(ROSA)26Sortm1.1(CAG-cas9*,-EGFP)Fezh/J mice (Jackson labs) and cultured in DMEM containing 20% heat inactivated FBS, Pen/Strep, and 30% L929-cell supernatant (bone marrow media, BMM) for 4 days before transduction with lentivirus.

For individual targeted gene knockouts, 25 bp oligos were synthesized by IDT containing the 20 bp protospacer sequences for individual genes. Paired sense and antisense sequences were annealed, 5' phosphorylated and double stranded cassettes cloned into pLenti-Puro vector (Addgene). gRNA sequences were chosen based on the outcome of the fold change effect seen in Brie library whole genome screening results. See table 1 supplementary materials for sequences. After correct sequence verification, HEK 293T cells were transfected with Lentiguide-puro vector containing individual gRNA sequences and helper vectors psPAX2 and pCMV-VSV-G. On day 2 and 3 post transfection viral supernatant was harvested and pooled.

References

1. Flannagan, R.S., V. Jaumouille, and S. Grinstein, *The cell biology of phagocytosis.* Annu Rev Pathol, 2012. **7**: p. 61-98.
2. Zhang, Y., A.D. Hoppe, and J.A. Swanson, *Coordination of Fc receptor signaling regulates cellular commitment to phagocytosis.* Proc Natl Acad Sci U S A, 2010. **107**(45): p. 19332-7.
3. Freeman, S.A., et al., *Integrins Form an Expanding Diffusional Barrier that Coordinates Phagocytosis.* Cell, 2016. **164**(1-2): p. 128-140.
4. Goodridge, H.S., et al., *Activation of the innate immune receptor Dectin-1 upon formation of a 'phagocytic synapse'.* Nature, 2011. **472**(7344): p. 471-5.
5. Lin, K.B., et al., *The rap GTPases regulate B cell morphology, immune-synapse formation, and signaling by particulate B cell receptor ligands.* Immunity, 2008. **28**(1): p. 75-87.
6. Batista, F.D., D. Iber, and M.S. Neuberger, *B cells acquire antigen from target cells after synapse formation.* Nature, 2001. **411**(6836): p. 489-494.
7. Grakoui, A., et al., *The Immunological Synapse: A Molecular Machine Controlling T Cell Activation.* Science, 1999. **285**(5425): p. 221.
8. Lin, J., et al., *TIRF imaging of Fc gamma receptor microclusters dynamics and signaling on macrophages during frustrated phagocytosis.* BMC Immunol, 2016. **17**: p. 5.
9. Allen, L.A. and A. Aderem, *Molecular definition of distinct cytoskeletal structures involved in complement- and Fc receptor-mediated phagocytosis in macrophages.* J Exp Med, 1996. **184**(2): p. 627-37.
10. Greenberg, S., K. Burridge, and S.C. Silverstein, *Colocalization of F-actin and talin during Fc receptor-mediated phagocytosis in mouse macrophages.* J Exp Med, 1990. **172**(6): p. 1853-6.
11. Ostrowski, P.P., et al., *Dynamic Podosome-Like Structures in Nascent Phagosomes Are Coordinated by Phosphoinositides.* Dev Cell, 2019. **50**(4): p. 397-410 e3.
12. Thornton, B.P., et al., *Analysis of the sugar specificity and molecular location of the beta-glucan-binding lectin site of complement receptor type 3 (CD11b/CD18).* J Immunol, 1996. **156**(3): p. 1235-46.
13. Rotty, J.D., et al., *Arp2/3 Complex Is Required for Macrophage Integrin Functions but Is Dispensable for FcR Phagocytosis and In Vivo Motility.* Developmental Cell, 2017. **42**(5): p. 498-513.e6.
14. Campellone, K.G. and M.D. Welch, *A nucleator arms race: cellular control of actin assembly.* Nat Rev Mol Cell Biol, 2010. **11**(4): p. 237-51.
15. Pollitt, A.Y. and R.H. Insall, *WASP and SCAR/WAVE proteins: the drivers of actin assembly.* Journal of cell science, 2009. **122**(Pt 15): p. 2575-2578.
16. Kumari, S., et al., *Actin foci facilitate activation of the phospholipase C-gamma in primary T lymphocytes via the WASP pathway.* Elife, 2015. **4**.
17. Takenawa, T. and S. Suetsugu, *The WASP-WAVE protein network: connecting the membrane to the cytoskeleton.* Nat Rev Mol Cell Biol, 2007. **8**(1): p. 37-48.
18. Suetsugu, S., T. Miki H Fau - Takenawa, and T. Takenawa, *Identification of two human WAVE/SCAR homologues as general actin regulatory molecules which associate with the Arp2/3 complex.* (0006-291X (Print)).
19. Shao, L., et al., *The Wave2 scaffold Hem-1 is required for transition of fetal liver hematopoiesis to bone marrow.* Nat Commun, 2018. **9**(1): p. 2377.
20. Ogaeri, T., et al., *The actin polymerization regulator WAVE2 is required for early bone marrow repopulation by hematopoietic stem cells.* Stem Cells, 2009. **27**(5): p. 1120-9.

21. Park, H., M.M. Chan, and B.M. Iritani, *Hem-1: putting the "WAVE" into actin polymerization during an immune response.* FEBS Lett, 2010. **584**(24): p. 4923-32.
22. Scott, B.L., et al., *Membrane bending occurs at all stages of clathrin-coat assembly and defines endocytic dynamics.* Nat Commun, 2018. **9**(1): p. 419.
23. Jongstra-Bilen, J., R. Harrison, and S. Grinstein, *Fcgamma-receptors induce Mac-1 (CD11b/CD18) mobilization and accumulation in the phagocytic cup for optimal phagocytosis.* J Biol Chem, 2003. **278**(46): p. 45720-9.
24. Dovas, A., et al., *Regulation of podosome dynamics by WASp phosphorylation: implication in matrix degradation and chemotaxis in macrophages.* J Cell Sci, 2009. **122**(Pt 21): p. 3873-82.
25. Linder, S. and P. Kopp, *Podosomes at a glance.* J Cell Sci, 2005. **118**(Pt 10): p. 2079-82.
26. Burns, S., et al., *Maturation of DC is associated with changes in motile characteristics and adherence.* Cell Motil Cytoskeleton, 2004. **57**(2): p. 118-32.

CHAPTER III. MINIMAL CLUSTERING OF FCγR REQUIRES ENDOCYTOSIS FOR SYK RECRUITMENT AND ACTIVATION: STRATEGIES FOR FCγR INHIBITION

Abstract:

Blocking Fcγ Receptor (FcγR) activation is an attritive therapy option for diseases involving autoreactive IgG immune complexes. Inhibitors are being developed that bind to the extracellular portions of FcγRs and preclude their binding to immune complexes and downstream activation of inflammatory responses. Currently the most potent FcγR inhibitor is a tri-valent Fc (SIF1) that binds FcγRs with high avidity and is retained on the cell surface. In contrast, a penta-valent Fc (PentX) can produce phosphorylated Syk kinase at low drug concentrations, indicating a delicate balance between the number of FcγRs needed for complete inhibition versus activation. Here, we have used a range of powerful fluorescent microscopy approaches to understand how these multivalent Fc molecules control FcγR microclustering and activation on the surface and within endosomes of macrophages. Surprisingly, single particle tracking by total internal reflection microscopy (SPT-TIRF) demonstrated that the motions of FcγRs docked with recombinant Fc (rFc), SIF1 or PentX, have display similar mobilities on the cell surface, characterized by medium-speed diffusion ($D \sim 0.15\ \mu m^2/s$) restricted to small domains on the plasma membrane. The rapid diffusion and analysis of spot amplitudes indicated that PentX/FcγR did not recruit additional downstream signaling molecules nor did they cluster into larger patches at the plasma membrane. SPT-TIRF showed that mScarlet-Syk was recruited transiently to the plasma membrane with nearly indistinguishable lifetimes. SIF1 and rFc showed modest rates of internalization and possible recycling to

the plasma membrane and did not retain Syk. However, internalized PentX accumulated on endosomes to which Syk was potently recruited. We conclude that at the plasma membrane, phosphatases maintain FcγRs in dephosphorylated state, that is indistinguishable for rFc and SIF1 and that endocytosis alleviates this inhibition enough for PentX, but not SIF1 or rFc to be phosphorylated. Thus, inhibition of FcγRs is achieved for low-valency Fc-multimers at both the plasma membrane and on endosomes.

Introduction

A hallmark of many autoimmune diseases is the presence of immunoglobulin G, IgG, autoantibodies and the formation of immune complexes (ICs). Recognition of ICs-associated IgG binding by the Fcγ receptor (FcγR) drives activation of macrophages which potentiates inflammation and autoimmune pathogenesis by the recruitment of other immune cells including neutrophils, monocytes, T cells, natural killer cells (NK cells), and additional macrophages [1, 2]. FcγR activation is therefore a recognized therapeutic target for disrupting autoimmunity.

The human FcγR family is comprised of activating (FcγRI, FcγRIIa, FcγRIIc, and FcγRIIIa) and inhibitory (FcγRIIb) receptors that tune FcγR immune response. Activating FcγRs signal via intracellular domains known as immunoreceptor tyrosine-based activation motifs (ITAMs) in the cytoplasmic tail of FcγRIIa and FcγRIIc or from an associated 'common gamma chain' (referred to as FcRγ) in FcγRI and FγcRIIIa. The inhibitory FcγRIIb contains an immunoreceptor tyrosine-based inhibition motifs (ITIMs). FcγRI is the high affinity receptor as it has three IgG like domains and bind IgG strongly ($Ka \sim 10^9$). FcγR activation and signaling occurs upon receptor engagement of an antibody-opsonized target, prompting receptor crosslinking, or clustering, and phosphorylation of the ITAM's phosphotyrosines by the Src Family Kinase, Lyn. Syk kinase is recruited to the ITAM's phosphorylated tyrosines and docks via its tandem SH2 domains [2-4]. Receptor clustering at the plasma membrane is thought to size exclude phosphatases and facilitate the necessary proximity of ITAMs for cross and auto-phosphorylation via Syk kinase [5, 6]. When FcγRIIb is engaged alongside activating FcRs, its ITIM becomes phosphorylated and it is thought to recruit SHIP or SHIP-1, SH2

domain-containing phosphatases, and acts as a negative regulator of the inflammatory responses that are triggered by ICs [2]. Downstream effects of FcγR activation include degranulation, oxidative burst, phagocytosis, antibody-dependent cell-mediated cytotoxicity (ADCC), and phagocytosis [1, 2, 7]. Activation of FcγRs by ICs initiates signaling for inflammation and autoimmunity which are a Syk and NFAT/NFkb dependent pathways [2].

In autoimmune pathogenesis, IgG-ICs, cause FcγRs to cluster and activate, and the resulting inflammatory response eventually culminates in tissue damage. IC autoimmune pathogenesis, such as in systemic lupus erythematosus (SLE), a chronic autoimmune disease that affects connective tissue, antinuclear antibodies cause ICs to deposit in various organs, begins when dying cells release autoantibodies and ICs during apoptosis [8]. Autoantibodies bind and stimulate B cells via the B Cell Receptor (BCR). The B cells reach full activation, becoming plasma B cells, when stimulated by T cells that are specific for the self-peptide. The plasma B cells produce more autoantibodies, which form more ICs and activate resident macrophages or newly arriving macrophages. Macrophages respond by either directly engaging the free ICs via the FcγR or by attempting to clear dying cells by phagocytosis [9]. However, in autoimmune diseases such as SLE, macrophages are unable to effectively clear the apoptotic cells and cells become necrotic. This leads to macrophage activation and a worsening of the disease [10]. Activated macrophages, whether by the ICs- FcγR clustering, or from necrotic cell components, release pro-inflammatory cytokines, IFN-β IL-12, IL-1B, and TNF-α (cytokines will vary based on activation pathway), that recruit and activate additional immune cells. Other downstream effects of the signaling pathways included

transcriptional regulation through ERK and Ca^{2+} NFAT pathways[4]. The recruitment of additional immune cells leads to escalated tissue damage, which leads to more autoantibodies to activate more B-cells leading to replenished populations of autoantibodies, creating a positive feedback loop that worsens the disease [10]. Macrophages also present antigen to cytotoxic T Cells, which promotes their activation and killing by perforin, granzymes, and granulysin [10]. This process wanes as ICs and apoptotic cells are eventually cleared by macrophages and waxes as B cells replenish autoantibodies and new ICs are formed.

SLE and RA are examples of an IgG-IC autoimmune disease where FcγR inhibition may be an effective therapeutic strategy. The most common manifestations of SLE include arthritis, renal damage, pleuritis or pericarditis, and skin rashes, which includes the butterfly, or malar, rash on the face [8]. As the inflammatory response cycles, so do the patients' symptoms. Interfering with FcγR activation by displacing autoantibody ICs can be an effective way to disrupt the cycle by inhibiting additional damage-inducing pro-inflammatory signals and preventing additional autoantibody production [11-14]. A second example is rheumatoid arthritis (RA), where the IgG-ICs similarly drive FcγR activation but resulting inflammatory response results in chronic joint inflammation that eventually culminates into tissue degradation and joint deformation [15]. The RA autoantibodies predominantly target rheumatoid factor and citrullinated peptides and are known to be primarily IgG [15]. Autoimmune pathogenesis involves networks of signaling pathways that can vary depending on the disease. However, a common feature of IC-driven autoimmune diseases like SLE and RA, is the FcγR activation caused by ICs which escalate the inflammatory response. Much of the

downstream inflammatory response could be avoided by preventing the binding of autoantibody ICs to the FcγR.

As a result of its association with autoimmunity, FcγR inhibition has been sought after as a therapeutic target for autoimmune diseases. Previous studies demonstrated the potential of FcγR inhibition as an efficacious therapeutic strategy to inhibit IC-associated autoimmune diseases [16]. Single IgG Fc fragments and IVIG have been used as effective therapeutics in animal rheumatoid arthritis models and in humans for various autoimmune diseases such as Kawasaki disease and acute immune thrombocytopenic purpura (ITP) [11-13]. While this strategy can provide therapeutic benefits, it requires large doses as the Fc-FcγR binding is 1-1 and may be displaced by polyvalent ICs. An alternative strategy, currently in clinical trial, is to create multivalent Fc molecules that have high affinity and avidity for the FcR, but do not activate it thereby providing a long-lived competitive inhibitor. By docking the FcγR with a higher avidity than the body's autoantibodies, the auto-ICs would be displaced. If the FcγRs are occupied but not activating, the pro-inflammatory response would be paused so fewer immune cells would cause inflammation and damage. Additionally, B cell would be prompted less to replenish autoantibody stores.

While a multivalent Fc is an ideal candidate for an inhibitor, an incomplete understanding of Fc valency and its effect on FcγR signaling has been an obstacle in multivalent Fc drug design. Prior work using engineered multivalent Fc molecules in varying valences and geometries has demonstrated that Fcγ molecules with a valency of five can drive activation, however three does not [14]. The pentameric construct in an X-geometry, PentamerX (PentX), acted as a strong agonist for FcγR activation while the

trimer, SIF1, had inhibited FcγR both in vitro as well as in multiple animal autoimmune models, including rheumatoid arthritis [14]. How these two constructs propagate such different cellular responses remains unknown and understanding their differences offers new insights into the mechanism of receptor activation.

Here, we applied a biophysical approach to understand how the multimeric Fc molecules influence FcγR activation and inhibition by using single molecule microscopy methods to interrogate clustering and Syk recruitment. Our findings shed new light on the importance of the geometric arrangement of FcγRs for their inhibition and activation by demonstrating that small clusters are competent for signaling by driving their rapid endocytic internalization and enabling signaling from endosomes.

Results

The mobility of FcγRs are largely unchanged by increasing valency.

Previously it has been shown that engineered molecules containing five Fcs in an x-configuration (PentX) can activate Syk [14], but molecules containing one Fc (rFc) or three Fcs arranged in a y-conformation (SIF1) cannot. Here, we sought to test the hypothesis that activation requires clustering of the FcRs at the cell surface and that five receptors is sufficient for this activation (PentX). Conversely, that three FcRs is not only insufficient, but precludes activation, providing a high-avidity, competitive inhibitor. We anticipated that the oligomerization state of the FcRs and their mobility on the cell surface could be detected using single particle tracking (SPT) [17, 18] of the labeled rFc, SIF1 and PentX (Fig. 3.1A). While SPT measurements have been routinely performed in epi-fluorescence mode using quantum dots at very low labeling density, we wanted an

approach that would access to molecular motions across a wide range of FcR occupancies. To satisfy this objective, we turned to total internal reflection fluorescence microscopy (TIRF) and a modification of our supported lipid bilayer approaches [19] to ensure that the glass substrate did not hinder the motions of the Fc molecules.

Cyclo RGD Supported Lipid Bilayers as a Tool for Particle Tracking

In order to study the free movement of FcγRs on the cell surface, we modified our previous SLB approach, that does not allow for macrophage attachment, to include the addition of cyclo RGD (cRGC) to allow macrophage attachment via integrins, but not activate FcγRs. A copper free click reaction using azide-alkine cycloaddition reaction, was used to react cRGD, with an attached azide, to liposomes containing the dibenzo-bicyclo-octyne (DBCO) component (Fig. 3.1B). The cRGD on the top leaflet of a the SLB offers an anchor point for integrin (Fig 3.1C). THP-1 cells were then exposed to multimeric Fcs on ice and then allowed to adhere to the SLB at 37 C for 30 minutes prior to imaging by SPT. Over 90% of cells bound to the cRGD bilayer, most cells created an enlarged contact zone and some cells had a smaller more punctate attachment zone (Fig. 3.1D). The contact zone of attachment and relative flatness was observed using DiI labeled THP-1 cells in TIRF and epifluorescence across 50 cells. Examples of interaction and non-interacting cells seen in TIRF are shown (Fig. 3.1E) and examples of cells treated with rFc DL594 demonstrate successful interaction with the bilayer (Fig. 3.1F).

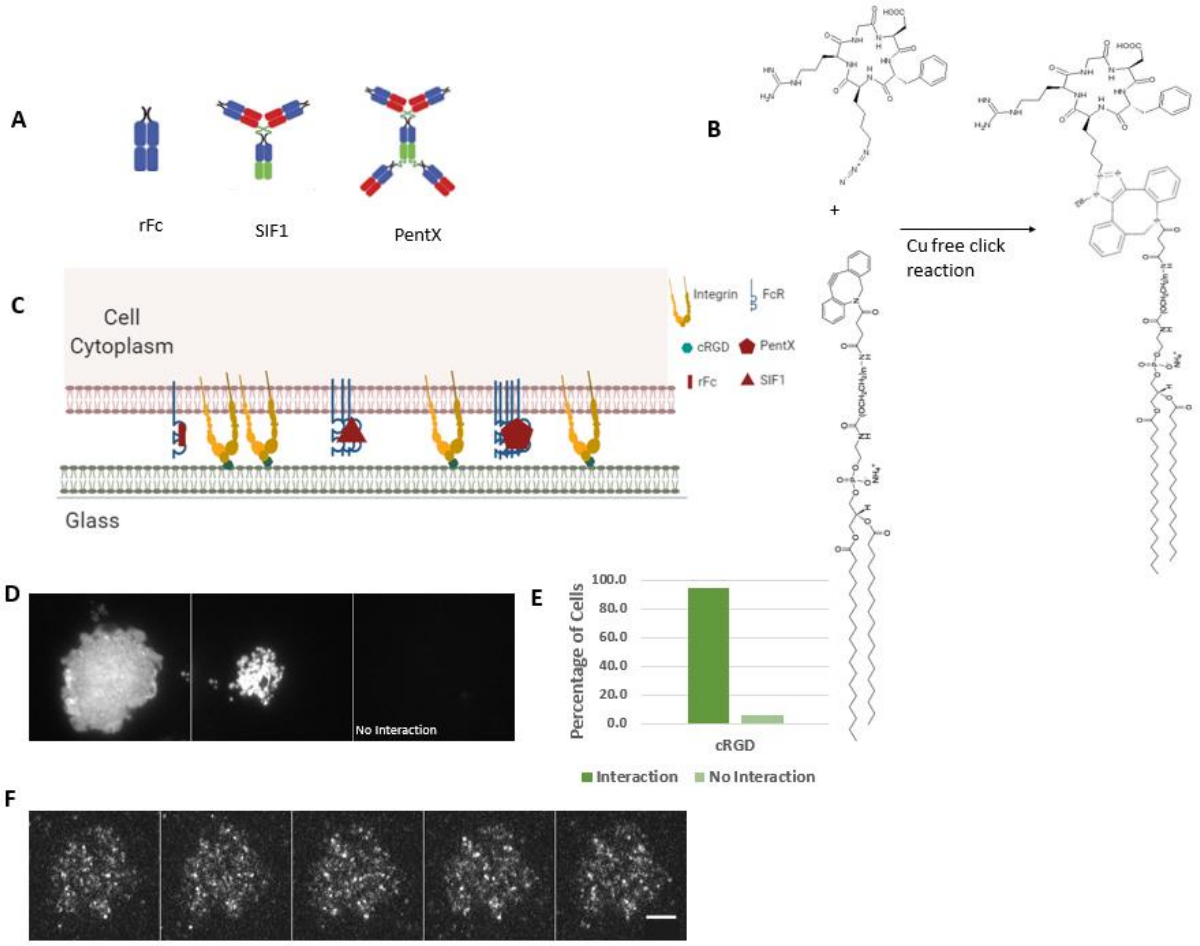

Figure 3.1 Cyclic RGD functionalized bilayers enable imaging of Fc-FcR interactions in context of low Fc construct dose. A) The Fc constructs used to study valency were rFc, SIF1, and PentX. Adapted from [14]. B) Liposomes are functionalized with cRGD using a Copper free click chemistry reaction between DSPE-PEG(2000) with a DBCO on it and a cRGD-azide. C) Illustration of bilayer showing the predicted engagement of integrins with cRGD functionalized bilayer and the possible Fc-FcR complexes. (Created with BioRender) D) Using the cRGD method, about 95% of THP1 cells show some level of interaction with the bilayer. This interaction varies in area but allows enough room to investigate the cell surface via TIRF microscopy. H) Cells labeled with DiI show this and are not visible in the TIRF field when they do not interact. F) Example of rFc DL594 cells interacting with cRGD bilayer. Scale bar represents 5um.

Fc valency has minimal effect on FcR mobility, even under activating conditions.

We anticipated that as the valency increased from one Fc (rFc), three Fcs (SIF1), to five Fcs (PentX) that 1) diffusion would slow as more FcRs were recruited and the

diameter of the complex increased and 2) activation of the FcR, by PentX, would recruit cytosolic molecules to the phosphorylated ITAMs leading to slowed diffusion and potential oligomerization of FcRs. The extent of slowing due to the engagement of multiple receptors is predicted by the Einstein-Stokes equation for a uniform medium as a function of particle radius in two-dimensions:

$$D = \frac{kT}{6\pi\eta a} \qquad Eq.1$$

where *a* is the radius of the complex and *k* is the Boltzmann constant, *T* is temperature, and η is the viscosity of the plasma membrane. Because all terms except *a* can be considered constants, then the diffusion coefficient scales as the inversed radius:

$$D \propto \frac{1}{a} \qquad Eq.2$$

In addition to frictional drag, diffusion can be slowed by barriers including interactions with the cytoskeleton and collisions with other surface proteins [20]. We first quantified the movements of DL594 labeled multimeric Fcs on the surface of PMA differentiated THP-1 cells adhered to cRGD-SLBs by TIRF microscopy. These movements were classified by their motion type. Classification of the motions of rFc, SIF1 and PentX using u-track, showed that SPT trajectories showed that all three constructs displayed predominantly free Brownian diffusion, and a significant fraction of confined diffusion and a small fraction of immobile molecules. Directed diffusion was negligible and excluded from further analysis. Representative SPT trajectories 2-dimensional for rFc using U-track that is color coded by the diffusion class is shown in Figure 3.2A (top). These same tracks are shown below with each track having a different

color to clearly show individual tracks. Figure 3.2B shows single representative tracks for confined, free, and immobile tracks. Under these conditions, low densities of Fc molecules allowed clear resolution of single particles on the cell surface (Fig. 3.2C). The bilayer condition was used to visualize individual Fc polymers at very low doses without the friction or drag the cell surface may experience on glass. Interestingly, the diffusion coefficients for the rFc, SIF1 and PentX single complexes were statistically indistinguishable (Fig 3.2D), indicating that that collisions with transmembrane proteins and other effects from the cytosol dominated the diffusion coefficients. This observation is surprising, since we anticipated being able to easily resolve the predicted 5-fold slower diffusion of PentX relative to rFc, at the sub-activating concentrations used. The average diffusion coefficients observed were close to those noted in literature, where free receptors diffused at a median rate of approximately $0.074 \pm 0.004\ \mu m^2$ per second when labelled with Cy3 [20].

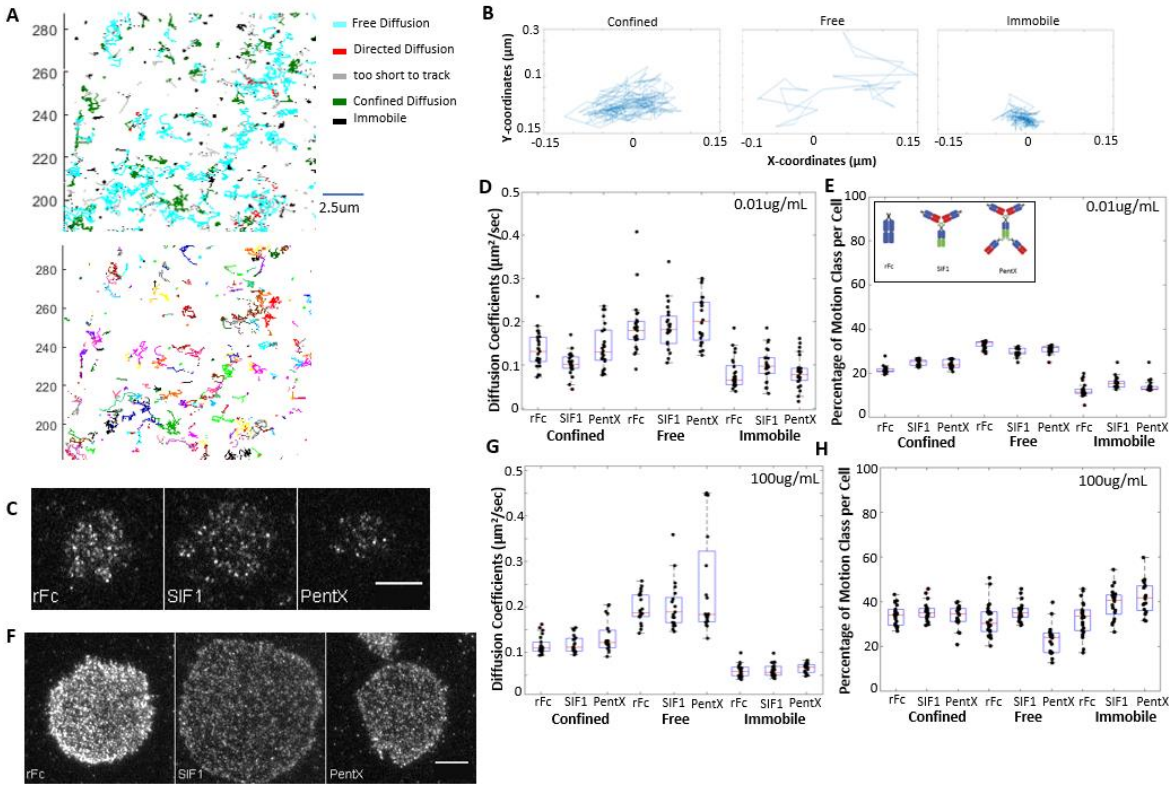

Figure 3.2 Fc valency has little impact on short range Fc/FcR diffusion. A) Representative of track classification of THP-1 cells treated with rFc. Top: Tracks color coded by diffusion class. Bottom: Tracks colors show individual tracks. B) Single tracks that fall within the confined, free, and immobile category. C) Representative images of cells treated with fluorescently labeled Fc constructs on SLBs in the non-activating dose, 0.7nM (0.03ug/mL rFc, 0.11ug/mL SIF1, and 0.17 ug/mL PentX). Scale bar represents 5um. D-E) Combined across three days of experiments. D) The average diffusion coefficient for cell track by diffusion class at non-activation dosages of (0.7nM). E) The percentage of tracks for each diffusion at sub activation dosages of 0.7nM (0.03ug/mL rFc, 0.11ug/mL SIF1, and 0.17 ug/mL PentX). F) Representative images of cells treated with fluorescently labeled Fc constructs on glass in an activating dose of 100ug/mL (about 0.4uM). G) The average diffusion coefficient for each cell by diffusion class at 100ug/mL (about 0.4uM). These are from a single experiment but are representative of data across multiple activating concentrations across multiple replicates. Scale bar represents 5um. H) The percentage of tracks for each diffusion class at 100ug/mL (about 0.4uM).

To delineate if FcR activation was associated with changes in mobility and oligomerization state, at fully activating (PentX) or inhibiting conditions (SIF1), THP-1 cells were exposed to 100 ug/mL concentrations of multimeric Fcs (Fig. 3.2F). Surprisingly, there were minimal differences in rate of diffusion across construct types or

relative to the low, sub-activating concentrations (Fig. 3.2G). The only distinguishable difference was an increase in the fraction of immobile complexes for each of Fc constructs (Fig. 3.2H). Given that these experiments were conducted on cleaned glass instead of the cRGD-bilayer, we cannot say with certainly if this was due to non-specific interactions with the glass or a characteristic change in the FcR complexes caused by the increased numbers of multimeric Fcs. Given that the increase was observed for rFc, as well as SIF1 and PentX, we believe that the increase in immobile fraction was due to interactions with the coverglass. The similar mobility for PentX was surprising given that receptor activation is generally associated with receptor immobilization such as in the case of the Fc epsilon receptor (FcεR) [21]. The negligible differences in distribution of free, confined, and immobile receptors as well as diffusion coefficients (Fig. 3.2E, Fig. 3.2H), indicates that FcγR mobility is controlled by physical barriers such as actin corrals, lipid rafts, and protein islands that result in receptors presiding in microdomains [20, 22, 23]. Pre-formed clusters of FcγRI were observed by super-resolution imaging in fixed cells that were perhaps corralled in by actin or lipid rafts [18]. If such pre-formed clusters were present, we would anticipate that our SPT data would show regions of confined diffusion with increasing numbers of overlapping Fc traces. Interestingly, our SPT traces showed zones of preferential occupancy and exclusion typically containing tracks from free and confined receptors with D ~ 0.15-0.2 $\mu m^2/s$ suggesting that rather than pre-formed clusters, the FcRs are corralled by actin [17, 18] but are able to diffuse within these zones. Indeed, observed confined diffusion trajectories had dimensions similar the cluster diameters ~ 50 nm observed for FcRI [18].

We applied Fluorescence Recovery After Photobleaching (FRAP) in TIRF to understand the effect of valency on diffusion over distances larger than could be accessed by SPT. Bleaching regions with a diameter of 3um (area of 7um^2) gave similar, slow diffusion coefficients with a weak trend of diffusion speeds of rFc> SIF1 > PentX (Fig. 3.3). The diffusion observed by FRAP, D~ 0.02-0.04μm^2/s, is about 5-10x slower than observed by SPT consistent with actin-corrals further restricting diffusion over portions of the membrane larger than 50 nm and therefore appearing slower than the SPT measurements. Interestingly, the mobile fraction across rFc, SIF1 and PentX were indistinguishable, indicating that even when PentX is present at concentrations known to activate Syk, the mobile fraction and diffusion of the FcR is not altered (Fig. 3.3C). Thus, FcR diffusion is slowed by interactions with the actin cytoskeleton at short range (SPT) and increasingly slowed over larger areas of the cell surface suggesting corralling within microdomains that limit their latera movement.

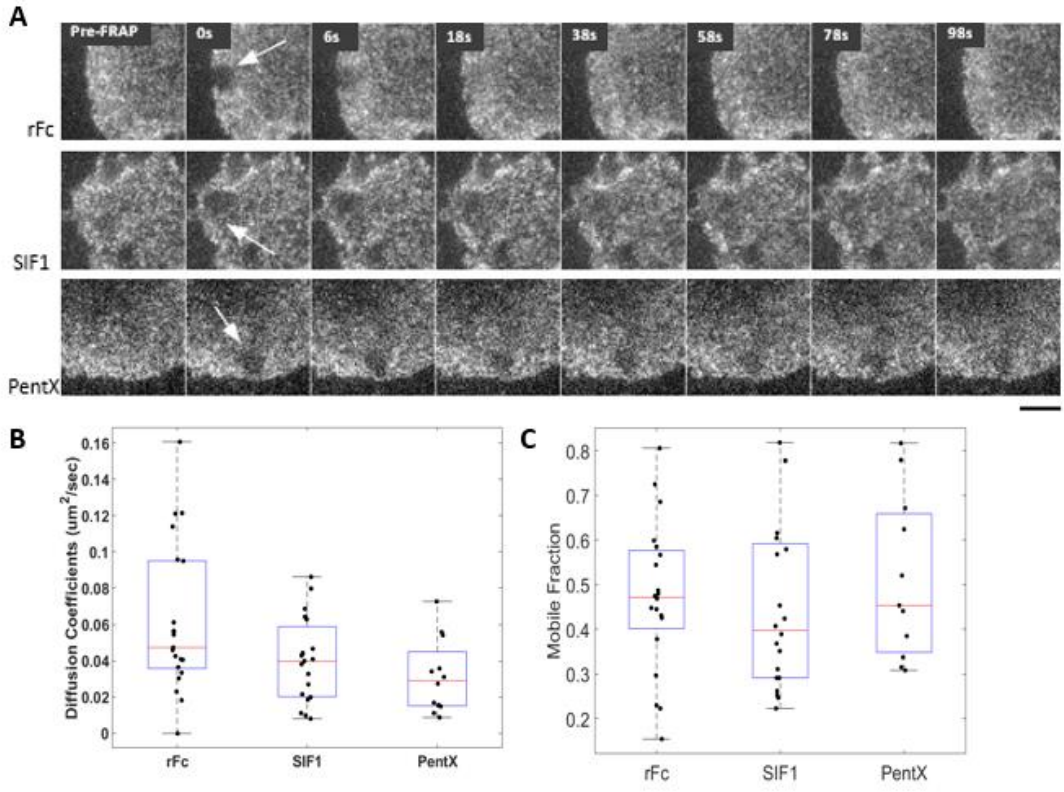

Figure 3.3 FRAP shows Fc Valency affects diffusion on larger length scale due to zones of confinement. A) Representative FRAP examples of rFc, SIF1, and PentX AF488 to show fast, medium, and slow recovery. The white arrows indicate the FRAP spot. Scale bar represents 5um. B) Average diffusion coefficients calculated from fluorescence recovery for 10 or more cells per condition for three replicates. C) Percentage of mobile fraction calculated from fluorescence recovery for 10 or more cells per condition for three replicates.

Two-color imaging indicates that FcγR receptors do not cluster on the plasma membrane even at activating concentrations of PentX.

Closely packed FcγRs form larger clusters once treated with polyvalent ICs consisting of DNP_{24}-BSA [18]. We tested to see if activating or inhibiting dosages of the multivalent Fc molecules would drive super clustering of the Fc bound receptors. To do so, THP-1 cells on glass were treated with the Fc molecules, rFc, SIF1, and PentX, that were tagged with either AF488 or DL594 in a 1:1 mixture (Fig. 3.4A-C). Timelapse

imaging revealed minimal colocalization of any of the molecules. Rather, receptors appeared to move around each other at random and remained segregated despite occasional collisions. This suggested that there is a distinction between small, mobile clusters that are not bound to an antigen, such as would have been the case in the cited literature where clusters aggregated together in the presence of DNP_{24}-BSA [18]. In that work, the super resolution imaging showed that human monocytes treated with DNP_{24}-BSA, bovine serum albumin labeled with 24 antibodies, formed clusters of 24 FcγRs that continued to oligomerize into even larger clusters. This may suggest a different mechanism of activation for small receptor clusters, possibly representing what occurs in some autoimmune diseases, that do not interact with large surface-associated antibodies.

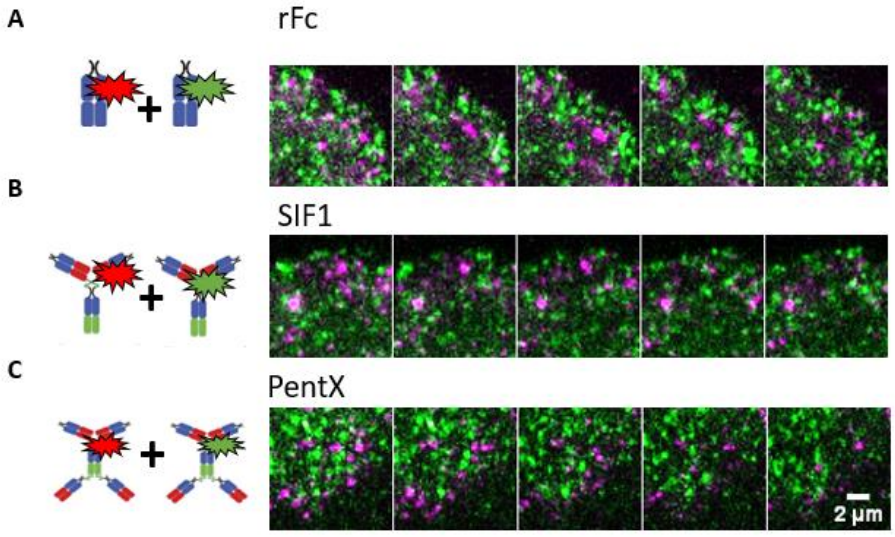

Figure 3.4 Small clusters do not form superclusters, even in activating concentration of PentX. A-B) Montages of cells treated with 33ug/mL rFc(A), SIF1(B), PentX(C) AF488 and 33ug/mL rFc (A), SIF1(B), PentX(C) DL594 over a timelapse of 40 seconds shows no long lasting colocalization of molecules. Adapted from [14].

FcγRs preferentially occupy small domains on the plasma membrane, but they are not pre-oligomerized.

Super resolution microscopy has been used to show that FcγRs pre-cluster on the cell surface in a process that depends on the actin polymerization state of the cell. Based on our observation that monomeric FcγRs, detected with rFc-DL594, had diffusion characteristics like that of three (SIF1) or five (PentX) FcγRs suggested that slow diffusion could be either due to micro-corralling of the receptors or the FcγRs existing in a pre-oligomerized state. To test these two possibilities, we performed an intensity analysis of our SPT data. If the fluorescent Fc molecules bound to FcγRs that were oligomerized or within very small microdomains (<~20nm) then single spots of increased brightness (or exhibiting multiple photobleaching steps) would be detected during high-density labeling of the FcγRs. Moreover, the brightness of rFc spots should be maximal since multiple rFc molecules will be bound at the sub-resolution spot and dimmer by ~1/3 for SIF1 and ~1/5 for PentX, as the number of FcγRs would limit the binding of Fcs. Alternatively, if the FcγRs diffuse within corrals, we would expect single spots of similar brightness for rFc, SIF1 and PentX that transiently diffuse into and out of sub-diffraction limited structures. Figure 3.5A shows rationale behind this approach, demonstrating that if each Fc molecule has one fluorophore the intensity of five receptors would be greatest for rFc, binding five individual receptors with five fluorophores, versus PentX which would bind five receptors to one Fc molecule, bearing one fluorophore.

To eliminate dynamics, cells were plated on glass and exposed to concentrations of Fc multimers but the same in total number of molecules. Treatment was done for five

minutes on ice followed by immediate fixation with 4% paraformaldehyde. This only allowed molecules to bind to the surface without the chance of internalizing. Each treatment condition was imaged under the same conditions. Representative images for each Fc molecule treatment are shown in Figure 3.5B. Point source detection in U-track was used to detect all the fluorescent spots (Fig 3.5C). The fluorescence intensities for each construct demonstrated spot brightness in the following order: rFc > SIF1 > PentX. However, the observed differences in intensity were approximately 4% and 13%, which are much smaller than the expected 1/3 and 1/5 intensities that would be expected for oligomerized receptors. Rather, we conclude that the smaller variance in intensity of the histograms correlates with the number of receptors within a larger ~ 50 nm corral and thus a reflection of a chance of coincident detection, similar what was observed in the 2-color experiments (Fig.3. 4). Both single and multi-step bleaching were indicating that some spots contained multiple fluorophores, however even at saturating concentrations the preponderance of spots in fixed cells corresponded to a left-skewed histograms that were highly similar amongst constructs suggesting that most spots reflect single Fc molecule's with occasional overlap with co-corralled neighbors (Fig. 3.5D-F).

To determine if the degree of clustering in live cells, spot amplitudes were averaged over the first four frames of the timelapse SPT represented in Figure 3.2. When comparing the mean spot per cell for the 0.01ug/mL and the 100ug/mL (Fig. 3.5G), histograms of the average spot intensities were nearly identical at the 0.01ug/mL and 100ug/mL across rFc, SIF1 and PentX indicating that FcγRs behaved as independent but corralled molecules. If oligomers were present, the low 0.01 ug/mL concentrations (Fig. 3.5H) should represent individual Fc molecules, whereas at high concentrations multiple

shoulders would be present in the 100ug/mL (Fig. 3.5I). However, the overall distribution reported a single population with only a small shoulder, likely reflecting the fact that occasionally multiple Fc molecules occupied the same spots. Although some cell to cell variance existed, the general trend points to a mostly homogenous population. This suggest the opposite of preclustered receptors. Rather, they were confined on the cell surface, but move independently as either single receptors, bound to rFc, or as clusters of three and five. Even in the case of activating PentX, clusters remain as independent, small mobile clusters that do not supercluster or change in motion type.

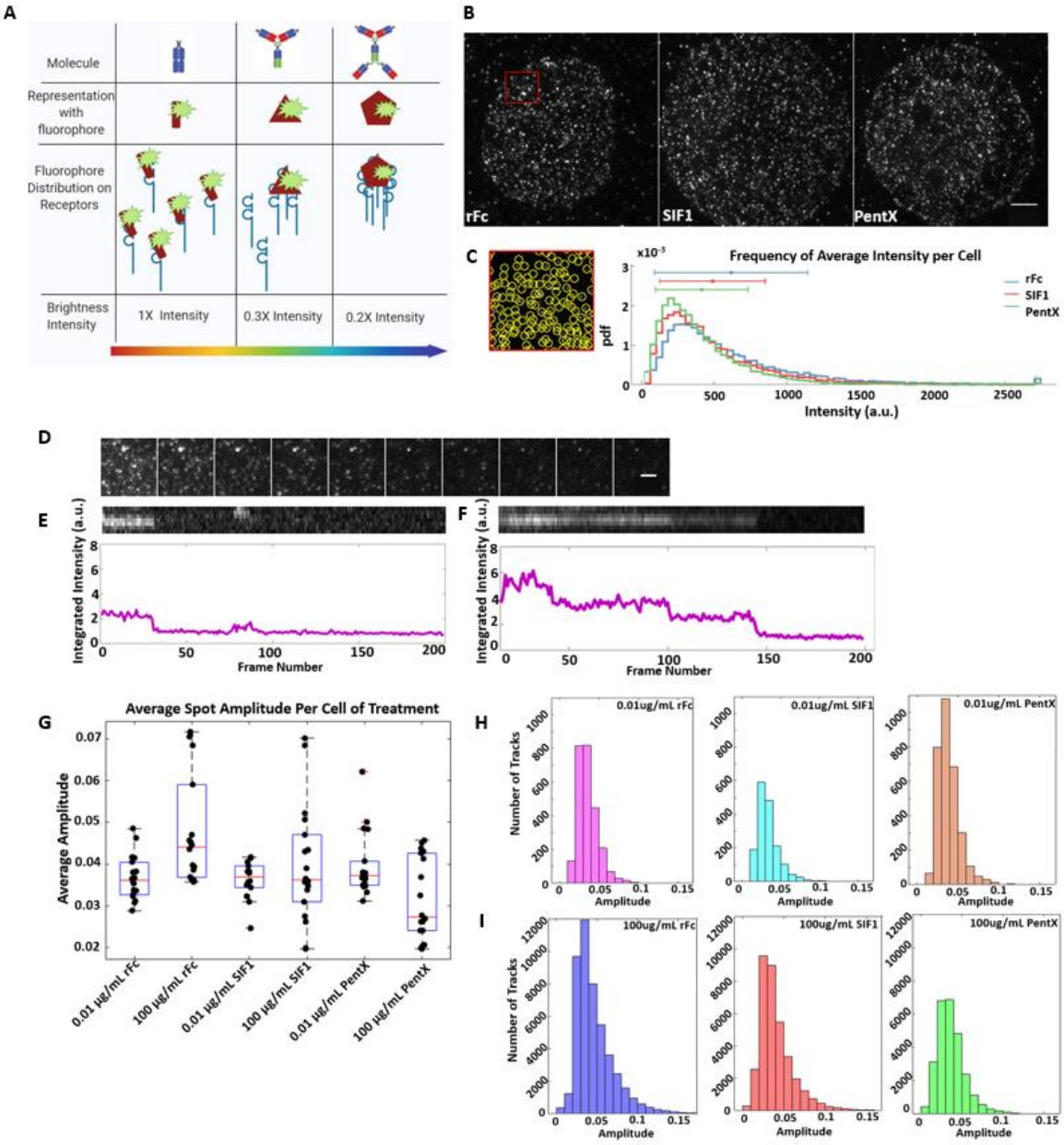

Figure 3.5 Fluorescence intensity analysis shows Fc receptors are not preclustered and remain in small, mobile clusters upon binding multivalent Fc. A) Schematic of Fc molecules and their fluorophore to FcγR ratio. (Created with BioRender) B) For intensity analysis, cells (represented in left) were treated with the same number/concentration of Fc molecules and fixed upon binding (Scale bar=5um). C) Fluorescent spot detection (left, zoomed in region from B) was used to plot the frequency of average Fc spot fluorescence at the same concentration (right). D) Sample of rFc bleaching over 200 frames that demonstrates stepwise bleaching (Scale bar=2um). E-F) Top: chymograph of predicted single (E) or multistep/fluorophore (F) bleach event. Bottom: Integrated intensity over time (frames) of above single (E) and multistep (F) bleached tracks. G) Average amplitude per cell taken over the first four frames of 100ug/mL and 0.01ug/mL dose multivalent Fc SPT data. H-I) Histograms of amplitude averaged over four frames for all tracks taken per Fc molecule treatment for 0.01ug/mL (H) and 100ug/mL conditions (I).

Pentamer drives rapid endocytosis and recruitment of Syk to endosomes.

In the case of phagocytosis, antibody/FcγRs engagement leads to rapid ITAMs phosphorylation at the plasma membrane by Src family kinase, Lyn, which creates a docking site for Syk, which in turn undergo auto and transphosphorylation for signal amplification. In the case of the FcεRI, intermediate and high antigen concentrations are correlated with immobilization and increased cluster sizes and rates of receptor internalization [21]. Previously it was shown that PentX drove rapid activation by Syk. We captured the dynamics of Syk-mScarlet recruitment at activating doses, 100ug/mL of AF488 conjugated multivalent Fc molecules. Imaging over the course of 45 minutes was done using Hi-Lo microscopy, a microscopy method that directs the laser at a glancing angle across the cell creating a confocal-like sectioning effect. Representative images of these data at approximately the same time after Fc treatment are found in Figure 3.6A. Confocal Z stack imaging was used to confirm that the that Hi-Lo imaging was accurately capturing cell cross-sections. This verified that PentX and Syk do colocalize in the same plane (Fig 3.6C). After being exposed to the multivalent Fc for 30 or more minutes, PentX was rapidly internalized and frequently colocalized with Syk at endosomes (Fig. 3.6B). Surprisingly minimal Syk recruitment to the PM was observed in PentX treatment, and rarely did it remain predominantly cytosolic after 30 minutes. SIF1 and rFc largely remained on the plasma membrane throughout the course of an hour, with only minimal internalization that could be associated with PM turnover. Syk remained in the cytosol under SIF1 and rFc conditions. SIF1 and rFc saw very little Syk recruitment and in the rare times that SIF1 or rFc were found in endosome, Syk was not

colocalized there. These observations are consistent with the previous observation that PentX is internalized over the course of one hour [14], but provide new insight into the fact that Syk is predominately recruited to FcγRs located within endosomes, but not the plasma membrane.

Syk is transiently recruited to and trafficked with PentX-FcγR, but not SIF1-FcγR

Given the observation that Syk was predominantly recruited to endosomes, we wanted to determine if activating FcγRs docked to multivalent Fcs would become phosphorylated and transiently recruit Syk, in a process that could be reversed by plasma membrane resident phosphatases. Using single particle tracking, we captured the recruitment dynamics of Syk-mScarlet to the plasma membrane and quantified the track length and positions at the cell surface. In all cases, flashes of Syk-mScarlet were observed, suggesting that Syk was transiently sampling receptors at the plasma membrane, but they exhibited little lateral movement (Fig. 3.D-E). Cumulative probability for track dwell time was calculated for tracks between 0.48 and 12 seconds (Fig. 3.6F). SIF1 and rFc had nearly identical cumulative probabilities most of which were less than 4 seconds or less in duration. The duration of Syk-mScarlet on the plasma membrane was slightly longer for PentX suggesting that this configuration may have afforded a few more activated ITAMs. However, the average Syk track length for rFc, SIF1, PentX were nearly identical, being 4.75 seconds, 4.73 seconds, and 4.89 seconds, respectively. Overall, we did not observe the anticipated extended tracks for Syk-mScarlet for PentX that we anticipated for an activation of FcγRs. We interpret these results to mean that at the plasma membrane, freely diffusing FcγRs docked with Fcs ranging in valency from 1-5 will collide with membrane associated phosphatases such as

CD45 that will rapidly deactivate them. Rather, it is only following endocytosis that PentX can fully activate the FcγRs and recruit Syk. SIF1 and rFc do not trigger this activation mechanisms and may be recycled to the plasma membrane.

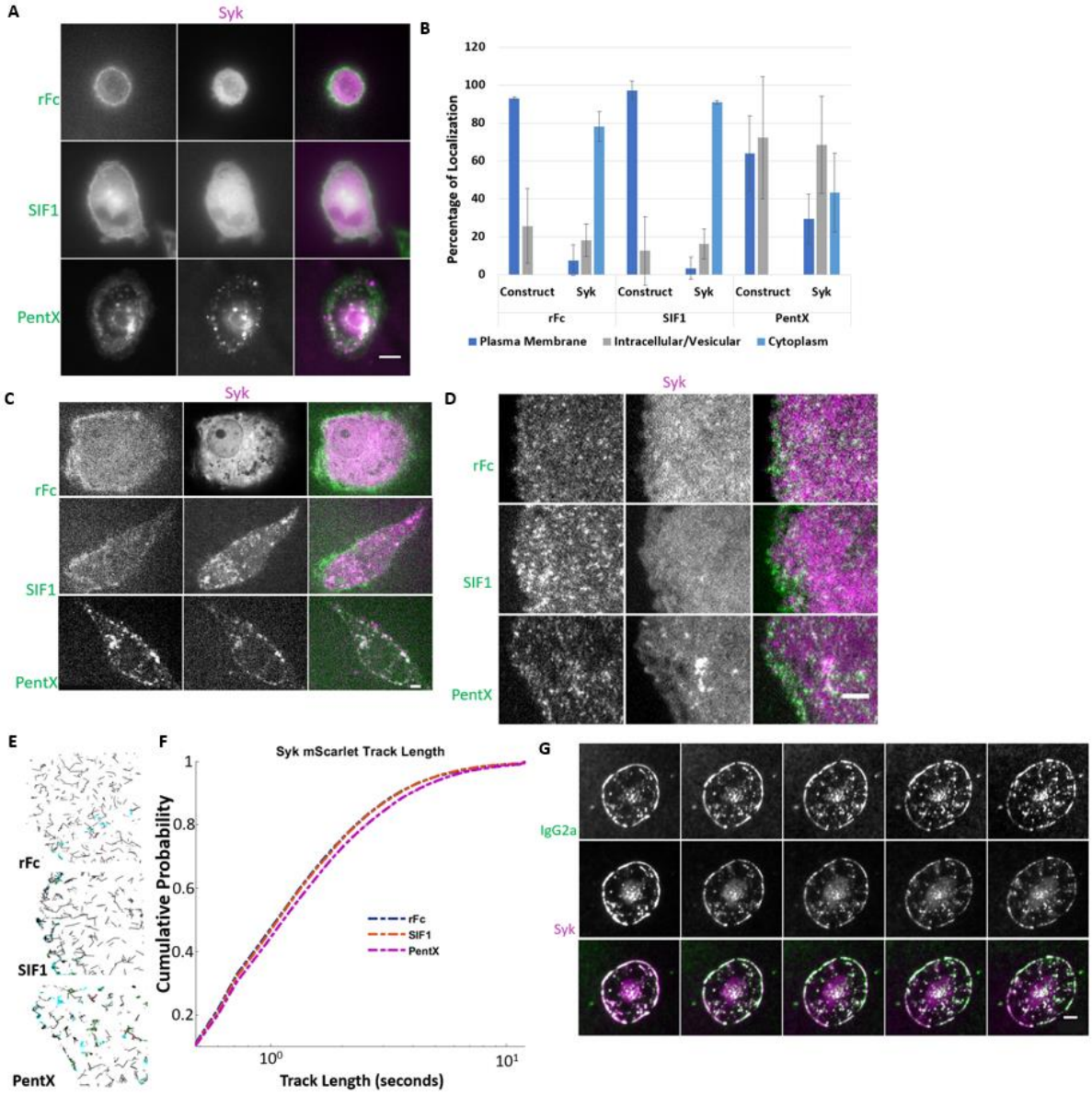

Figure 3.6 PentX prompts Syk recruitment to endosomes rather than the PM. A) The localization of Fc molecules and Syk using Hi-lo images show Syk localization at endosomes containing PentX (images represent 30 minutes post 100ug/mL treatment). Scale bar represents 5um. B) Hi-lo data from A was quantified as the percentage of localization for Fc molecules and Syk localization. The data was taken over the course of 45 minutes post treatment and represents three different days of experiments and approximately 50 cells for each Fc treatment. C) Confocal images of 100ug/mL Fc molecule treated Syk-mScarlet THP-1 cells verify colocalization of Syk at PentX endosomes. Scale bar represents 2um. D) TIRF timelapse imaging of Syk-mScarlet cells treated with AF488-Fc molecule treatment was used for tracking Syk (scale bar represents 3um). E-F) 2D Syk tracks, colored by classification, show little lateral movement. (Cyan=free diffusion, green=confined diffusion, black=immobile) (E). Track length cumulative probability showed a minor increase in Syk residency at the plasma membrane (F). G) Representative data of THP1 Syk-mScarlet interaction on a an IgG2a-AF647 opsonized bilayer shows recruitment of Syk to IgG-FcγR clusters. Scale bar represents 3um.

To compare this result with surface-associated antibody, a supported lipid bilayer opsonized with IgG2a-AF647, described in [19], was used to image Syk dynamics. Here, Syk-mScarlet expressing THP-1 cells were dropped on the bilayer and time-lapse images of receptor engagement were captured. The THP-1 cells engaged the IgG and Syk rapidly co-localized at the leading edge of a newly formed and advancing pseudopod. Additionally, Syk also relocated to the PM near receptor engagement (Fig.3.6F) [19]. Thus, we conclude that while FcR clustering by multivalent Fcs of 5 is capable of activating Syk, this response occurs on endosomes (Fig. 3.7) and is distinct from the activation mechanisms at the plasma membrane which require a particle to displace opposing phosphatase inhibition.

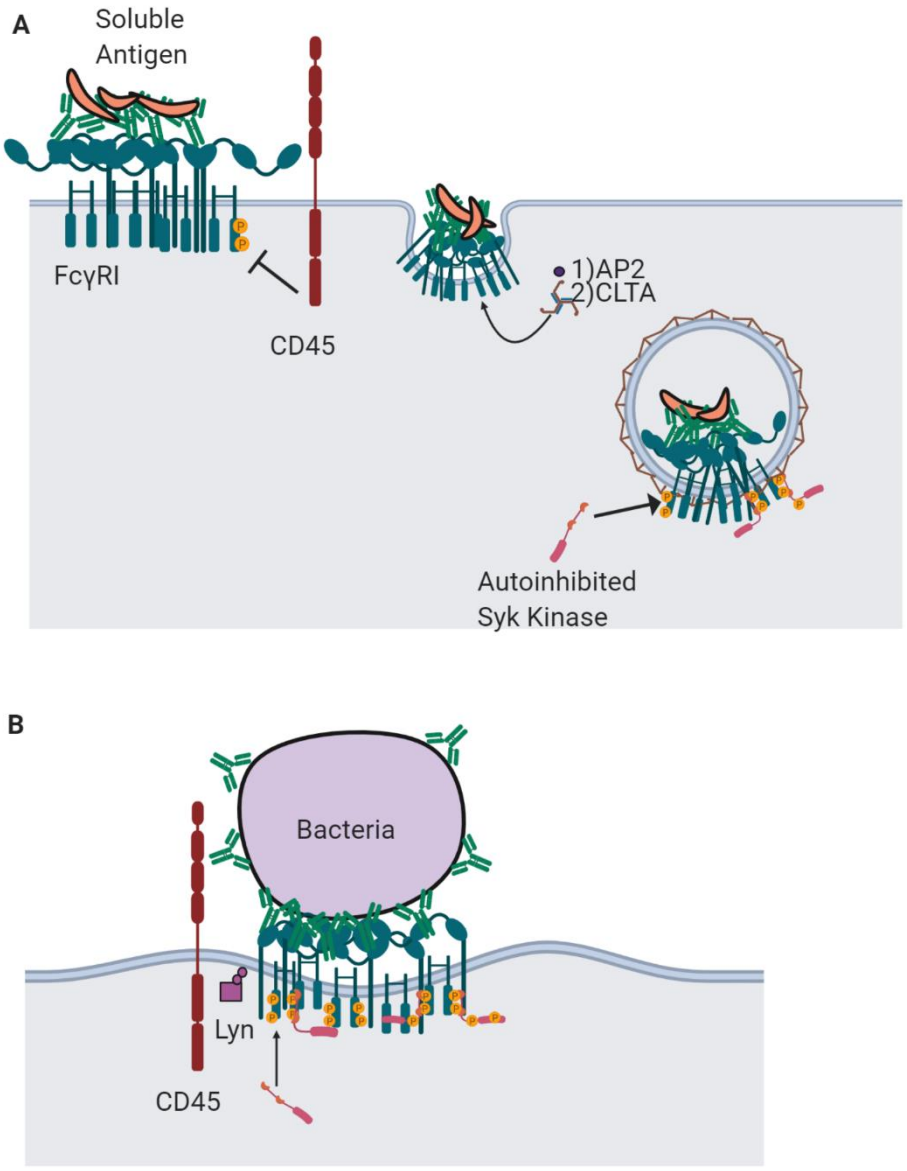

Figure 3.7 Proposed model of soluble IC: FcγR endosomal activation versus surface-associated antibody FcγR activation A) Proposed mechanism for FcγR activation in the context of small clusters formed via soluble antigen ICs. IC: FcγR cluster are rapidly dephosphorylated by tall phosphatases but signal for AP2 clathrin adaptor followed by clathrin triskelia which internalized the small clusters where they can recruit Syk and promote inflammatory signal. B) FcγR activation in the context of surface-associated antibody that docks FcγRs and forms clusters that create a tight space where CD45 cannot fit. Dual tyrosines of the ITAM are phosphorylated by Lyn. Syk is recruited to the phosphotyrosines resulting in amplified signal that leads to downstream immune response such as phagocytosis. (Created with BioRender)

Discussion

The designer multimeric Fc molecules, rFc, SIF1, and PentX, provided new fundamental mechanistic insight into the minimal number of FcγRs necessary to form and activate signaling complexes. This work indicates that the molecular environment contributes to this minimum threshold. Specifically, our data demonstrated that PentX, which potently drives Syk phosphorylation through the binding of five FcγRs [14], requires compartmentalization of the PentX/FcγR complex to recruit Syk. This is a sharp contrast with freely mobile surface associated IgG, which potently recruits Syk to the plasma membrane. Taken together, these results are fully consistent with the proposed models for FcR activation that require segregation of the FcγRs from phosphatases to allow full activation. At the plasma membrane, it is thought that rearrangements of the actin cytoskeleton and potentially the activation of integrins mediate that sorting, when surface associated IgG/FcγR interactions limit the spacing between the phagocyte membrane and target, thereby excluding bulky and glycosylated phosphatases such as CD45 [20, 24] by forming physical barriers [20, 25, 26]. In contrast, PentX and potentially soluble immune complexes do not create a sufficient rearrangement of the cell surface to provide this segregation and thus, five FcγRs is insufficient to trigger Syk activation at the plasma membrane. Moreover, our measurements demonstrated that multimeric FcγR clusters, even in activating conditions, remain predominantly mobile on the plasma membrane and are corralled in regions that may be enriched in phosphatases that suppress activation. Thus, in contrast to phagocytosis, the five FcγRs appear insufficient to drive actin cytoskeleton facilitation of receptor clustering [17], but this

does not preclude FcγR activation on endosomes. This strongly implies a signaling mechanism unique to small, soluble IC: FcγR complexes.

Within the observed behaviors of these three Fc molecules, the endocytosis was PentX's most distinguishing feature [14]. In contrast to conventional thinking, endocytosis in this system does not appear to be a result of Syk recruitment to ligated FcγRs, but rather that endocytosis provides a microenvironment for FcγR signaling and Syk recruitment. It remains unclear if the multivalent Fcs promote endocytosis and subsequent Syk recruitment or if endocytosis of the Fc/FcγR complexes is a default pathway and through the removal of the complex from the plasma membrane, FcγR activation occurs. Our data suggest that in the case of SIF1 and rFc, no detectable Syk recruitment is observed on internal membranes or the plasma membrane, despite endocytic traffic of SIF1 and rFc. Furthermore, the long residency time of SIF1 and rFc on the cell surface, suggests that these molecules docked to FcγRs are dynamically being internalized and recycled back to the cell surface. Important future work will include determining if FcγR clusters of greater than five can signal for endocytosis. A potential mechanism for this would be that following clustering, the FcRγ is capable of recruiting clathrin-associated sorting proteins (CLASPs) that drive endocytosis. Markers for endocytosis would be the YXXØ or [DE]XXXL[LI] [27]. Of those motifs, YXXØ occurs multiple times throughout the FcRγ, of which the tandem YXXL motifs of the ITAMS fall within this classification.

This work also provides insights into how SIF1 works as an inhibitor. While capable of binding three FcγRs, it appears to behave identical to rFc, suggesting it is not recognized by activation machinery. This was demonstrated by the lack of observed

colocalization with Syk kinase packaging into endosomes for degradation. Additionally, there was no discernable effect on receptor mobility and rearrangement on the cell surface, which suggests that it behaves as an ideal competitive inhibitor. In summary, SIF1 as an inhibitor is capable of docking three FcγRs while maintaining the properties of a single receptor which makes it ideal to displace auto-antibodies.

In conclusion, we have demonstrated that small, mobile clusters of five FcγRs are signaling competent but in a mechanistically distinct way than that of surface-associated antibody targets. Rather, they are not free of collisions with phosphatases and consequential dephosphorylation until being endocytosed. Once trafficked on endosomes, the clusters of five can enhance signaling by recruiting cytosolic Syk kinase. These findings represent a new mechanism of FcγR activation that is unique to soluble IC: FcγR activation and provides insights into autoimmune pathogenesis. Moreover, SIF1's inability to signal for endocytosis illustrates its worth as an inhibitor.

Methods

THP-1 cell culture and differentiation.

THP-1 cells were cultured in RPMI-1640 Medium (ATCC 30-2001) and maintained at 100,000-200,000 cells per milliliter. THP-1 differentiation was done using Phorbol 12-myristate 13-acetate, 97% from Acros Organics (AC356150010) to create human monocytes capable of adherence and behave similarly to macrophages. THP-1 cells were spun down at 12000 rpm for 4 minutes and plated in a six well dish containing about 200,000 cells per mL in RPMI containing 50 ng/mL PMA for 48hours. After 48 hours, cells rested for 24 hours in RPMI, no PMA. PMA was diluted by adding 10uL of 1mg/mL DMSO frozen stock into 240uL of DMSO or RPMI (for a 40ng/uL solution), 5uL of this stock was then added to well of the 6-well dish for a final 50ng/mL. For imaging cells on glass, cells were differentiated directly on ethanol flamed 25 mm coverslips (Number 1.5) (Thermo Fisher) or onto -6 well glass bottom plates (dot scientific) (MGB096-1-2-LG-L) for high content experiments.

Characterizing PMA differentiated Cells

PMA Differentiated THP-1 cells were characterized using fluorescently conjugated Fab fragments of hCD64 (Santa Cruz Biotechnology sc1184) and hCD32 (StemCell Technologies 60012). Fab fragments were generated using 62.5 ug of each antibody in the Pierce Fab micro preparation kit (Thermofisher 44685) for a four-hour reaction and then stopped at 5000g for one minute. 15uL of each sample was mixed with the 5x non-reducing SDS buffer and loaded onto a 12% SDS page gel (Biorad) and ran for 30 minutes at 230 volts. Coomasi blue staining was used to visualize lanes.

The CD64 and CD32 fab fragments were labeled with AF647 NHS ester and used to label THP-1 and differentiated THP-1 cells. Cells were blocked with dPBS+1%FBS for 15 minutes on ice before adding the fab fragments diluted into dPBS with 1%FBS at a 1:8 dilution of 1.14uM labeled fab fragments (final of approximately 0.18uM) incubated 20 minutes on ice, spun down at 800g for 3 minutes and resuspended in cold HBSS and kept on ice until analyzed by the BD Accuri C6 flow cytometer. Flow cytometry data revealed in increase in CD64 and CD32 expression.

To validate if the PMA differentiated cells behaved like macrophages, cells on plastic underwent a sheep red blood cell uptake assay to validate their ability to phagocytose similarly to macrophages. A 30:1 MOI of biotinylated and anti-IgG2a sRBCs were dropped on differentiated THP1 cells and phase contrast microscopy using an inverted fluorescent microscope was done for a qualitative analysis of THP-1 cells ability to phagocytose.

Live Cell imaging

The PMA treated THP-1 cells plated on coverslips and were imaged in AttoFluor chambers (ThermoFisher) using TIRF-based imaging which was conducted with an inverted microscope built around a Till iMic (Till Photonics, Germany) equipped with a 60 × 1.49 N.A. oil immersion objective lens, enclosed in an environmental chamber to keep the samples at 35–37 °C using heater fans. The entire microscope setup and centering of the back focal plane was previously described in [28]. Excitation for TIRF was provided by either a 561 nm laser, for DL594 labeled molecules or Syk-mScarlet or a 488nm laser for the AF488 labeled molecules. Single point TIRF was used for fast imaging of single particles while TIRF 360 was used to create uniform TIRF illumination

for moderate speed particle tracking and fluorescence recovery after photobleaching (FRAP) by steering the laser at the back-focal plane. The microscope was custom-built based on iMIC system (TILL Photonics, Munich, Germany) with 60x 1.49 oil immersion objective lens (Olympus, Tokyo, Japan).

Spinning disk confocal experiments of the Syk-mScarlet cells were done using a 561 laser to excite the mScarlet and the AF488 Fc molecules were imaged with a 445nm laser. This is not an ideal laser for excitation, so Hi-Lo was relied on for increasing 'n' for these data.

Supported Lipid Bilayer formation

Supported lipid bilayers were formed by spontaneous fusion of lipid vesicles. For the bilayers DSPE-PEG(2000) Biotin (Avanti Polar Lipids 880129)or DSPE-PEG(2000)-DBCO (Avanti Polar Lipids 880229) and POPC Avanti Polar Lipids (850457) were mixed at a molar ratio of 1:100 with total lipid concentration of 500μM. The lipid mixture was then dissolved in chloroform and dried using a vacuum centrifugation to remove the chloroform, where the first minute ran at 30C and the remaining temperature was set to room temp. The lipid film was re-suspended in dPBS by initially vortexing and then sonicating for 5 min using a bath sonicator and then extruded through (Avanti Polar Lipids 610000) 100 nm filter at least 13 times (Whatman Nucleopore Track-Etch 100nm membrane**)**. For the cRGD bilayer, 10uL of 0.1mg/mL cRGD-azide (1ug) (Peptides International 004327) added to the solution prior to vortexing. The bilayer was formed on Piranha acid (H_2SO_4 (30 %, ***v/v***):H_2O_2 (3:1, ***v/v***)) cleaned coverslips and then dunked in water at about 42C to remove excess liposomes. The water was exchanged with dPBS

followed by Hank's balanced Salt Solution for either imaging (Corning). The bilayer coated coverslip was kept in a buffer solution during washing and transferring to imaging chamber to protect SLB from drying out and to keep it uniform. For opsonization of the biotinylated bilayers, Alexa Fluor 647 NHS ester (Thermofisher Invitrogen) was conjugated to anti-Biotin IgG (clone 3E6) for antibody fluorescent labeling. The labeled antibody was incubated with the 0.1% PEG-biotin SLB at 37 °C for 30 min. Excess IgG was washed with imaging buffer.

Single and Multivalent Fc Treatments

The designer Fc molecules, rFc, SIF1, and PentX were provided by Momenta Pharmaceutical as part of a collaboration. For the low dosage on bilayers, single particle assays on the cRGD bilayer, differentiated THP-1 cells were removed from the plastic dish using cold dPBS and then treated in suspension at 4C with either 0.03ug/mL rFc-DL594, 0.11ug/mL SIF1-DL594, or 0.17ug/mL PentX-DL594. This dosage is approximately 1.4nM for each construct and should not be activating according to [14]. Treatment on ice was done for 30 minutes and then cells were washed and resuspended in HBSS and dropped on the supported lipid bilayers. For each construct treatment, about 200,000 cells were used, of which about 120,000 cells were dropped onto the supported lipid bilayer.

For moderate and high dosage treatments on glass, Fc constructs labeled with AF488 were used at the same mass 33ug/mL, 66ug/mL, or 100-110ug/mL doses for the particle tracking data. For the two-color Fc experiments, 33ug/mL of AF488 and 33ug/mL of DL594 were mixed and cells were treated with them at the same time as in

the single-color Fc treatments. These were treated at 37C for 5 minutes and then washed and imaged immediately over the course 45 minutes after washing. For brightness analysis, Fc constructs were all 0.4uM for each to keep the total number of molecules the same for each. These experiments were done with cells on glass. Predominately cells were differentiated directly on glass, but in some cases, cells were removed from a plastic dish and plated on ethanol flamed coverslips and allowed to adhere at least overnight. For each of these, ideally 150,000-200,000 cells per coverslip were plated.

Image Processing

Fiducial data collection and image registration: Single images were registered using calibration images acquired simultaneously on each of the four EMCCD detectors. A single image of 200 nm green beads (Life Technologies, Carlsbad, CA) immobilized on a glass coverslip were excited using 445 nm excitation. Coordinates for registration were determined using the MATLAB (The MathWorks, Inc., Natick MA) cpselect tool. A rigid affine transformation was used to transform all points onto the red channel.

Image montages were generated using ImageJ, and due to unintended photobleaching in some data sets, the Bleach Correction tool was used (Kota Miura et al. (2014). ImageJ Plugin CorrectBleach V2.0.2. Zenodo. 10.5281/zenodo.30769).

U-track (Danuser Lab) was used for single particle tracking using the Gaussian detection [29, 30]. For the brightness analysis and syk kinase track length, point source detection without tracking was used. Data was extracted and visualized using both customized codes and provided, for plotting 2D tracks by classification.

THP-1 syk-mScarlet lentiviral transduction

To produce lentivirus, $3x10^6$ 293T cells were seeded in a 6-well treated 10 cm plates. The next day after plating, each dish was transfected with 6ug gRNA Syk-mScarlet-pLJM1, 6ug psPAX2, 1ug pVSVG, and 24 uL of 1 mg/mL polyethylenimine (PEI). After 48 hours, lentivirus was harvested, centrifuged, and aliquoted into 15 mL tubes and stored at -80C or -150C. For lentivirus transduction into THP1 cells, cells were transduced using the harvested virus for 48 hours. After the 48hour transduction, cells were selected with Blasticidin (10ug/mL) for two days. THP-1 cells were transduced using 200,000 cells per well of a 6-well plate.

References

1. Nimmerjahn, F. and J.V. Ravetch, *Fcγ receptors as regulators of immune responses.* Nature Reviews Immunology, 2008. **8**: p. 34.
2. Li, X. and R.P. Kimberly, *Targeting the Fc receptor in autoimmune disease.* Expert Opin Ther Targets, 2014. **18**(3): p. 335-50.
3. Lowell, C.A., *Src-family and Syk kinases in activating and inhibitory pathways in innate immune cells: signaling cross talk.* Cold Spring Harb Perspect Biol, 2011. **3**(3).
4. Mocsai, A., J. Ruland, and V.L. Tybulewicz, *The SYK tyrosine kinase: a crucial player in diverse biological functions.* Nat Rev Immunol, 2010. **10**(6): p. 387-402.
5. Flannagan, R.S., V. Jaumouille, and S. Grinstein, *The cell biology of phagocytosis.* Annu Rev Pathol, 2012. **7**: p. 61-98.
6. Goodridge, H.S., et al., *Activation of the innate immune receptor Dectin-1 upon formation of a 'phagocytic synapse'.* Nature, 2011. **472**(7344): p. 471-5.
7. Zhang, Y., A.D. Hoppe, and J.A. Swanson, *Coordination of Fc receptor signaling regulates cellular commitment to phagocytosis.* Proc Natl Acad Sci U S A, 2010. **107**(45): p. 19332-7.
8. Cojocaru, M., et al., *Manifestations of systemic lupus erythematosus.* Maedica, 2011. **6**(4): p. 330-336.
9. Murphy, K.W., Casey, *Janeway's Immunology*. Vol. 9. 2017, New York and London: Garland Science Taylor and Francis Group. 924.
10. Ushio, A., et al., *Crucial roles of macrophages in the pathogenesis of autoimmune disease.* World Journal of Immunology, 2017. **7**(1).
11. Anthony, R.M., et al., *Recapitulation of IVIG Anti-Inflammatory Activity with a Recombinant IgG Fc.* Science, 2008. **320**(5874): p. 373-376.
12. Debré, M., et al., *Infusion of Fcγ fragments for treatment of children with acute immune thrombocytopenic purpura.* The Lancet, 1993. **342**(8877): p. 945-949.
13. Oates-Whitehead, R.M., et al., *Intravenous immunoglobulin for the treatment of Kawasaki disease in children.* Cochrane Database Syst Rev, 2003(4): p. CD004000.
14. Ortiz, D.F., et al., *Elucidating the interplay between IgG-Fc valency and FcγR activation for the design of immune complex inhibitors.* Science Translational Medicine, 2016. **8**(365): p. 365ra158.
15. Schellekens, G.A., et al., *Citrulline is an essential constituent of antigenic determinants recognized by rheumatoid arthritis-specific autoantibodies.* The Journal of clinical investigation, 1998. **101**(1): p. 273-281.
16. Flaherty, M.M., et al., *Nonclinical evaluation of GMA161--an antihuman CD16 (FcgammaRIII) monoclonal antibody for treatment of autoimmune disorders in CD16 transgenic mice.* Toxicol Sci, 2012. **125**(1): p. 299-309.
17. Jaumouille, V., et al., *Actin cytoskeleton reorganization by Syk regulates Fcgamma receptor responsiveness by increasing its lateral mobility and clustering.* Dev Cell, 2014. **29**(5): p. 534-546.
18. Brandsma, A.M., et al., *Mechanisms of inside-out signaling of the high-affinity IgG receptor FcγRI.* Science Signaling, 2018. **11**(540): p. eaaq0891.
19. Lin, J., et al., *TIRF imaging of Fc gamma receptor microclusters dynamics and signaling on macrophages during frustrated phagocytosis.* BMC Immunol, 2016. **17**: p. 5.
20. Freeman, S.A., et al., *Integrins Form an Expanding Diffusional Barrier that Coordinates Phagocytosis.* Cell, 2016. **164**(1-2): p. 128-140.
21. Andrews, N.L., et al., *Small, mobile FcepsilonRI receptor aggregates are signaling competent.* Immunity, 2009. **31**(3): p. 469-79.
22. Horejsi, V. and M. Hrdinka, *Membrane microdomains in immunoreceptor signaling.* FEBS Lett, 2014. **588**(15): p. 2392-7.

23. Garcia-Parajo, M.F., et al., *Nanoclustering as a dominant feature of plasma membrane organization.* Journal of Cell Science, 2014. **127**(23): p. 4995-5005.
24. Bakalar, M.H., et al., *Size-Dependent Segregation Controls Macrophage Phagocytosis of Antibody-Opsonized Targets.* Cell, 2018. **174**(1): p. 131-142 e13.
25. Ostrowski, P.P., S. Grinstein, and S.A. Freeman, *Diffusion Barriers, Mechanical Forces, and the Biophysics of Phagocytosis.* Dev Cell, 2016. **38**(2): p. 135-46.
26. Grakoui, A., et al., *The Immunological Synapse: A Molecular Machine Controlling T Cell Activation.* Science, 1999. **285**(5425): p. 221.
27. Traub, L.M. and J.S. Bonifacino, *Cargo recognition in clathrin-mediated endocytosis.* Cold Spring Harb Perspect Biol, 2013. **5**(11): p. a016790.
28. Scott, B.L., et al., *Membrane bending occurs at all stages of clathrin-coat assembly and defines endocytic dynamics.* Nat Commun, 2018. **9**(1): p. 419.
29. Jaqaman, K., et al., *Cytoskeletal control of CD36 diffusion promotes its receptor and signaling function.* Cell, 2011. **146**(4): p. 593-606.
30. Jaqaman, K., et al., *Robust single-particle tracking in live-cell time-lapse sequences.* Nat Methods, 2008. **5**(8): p. 695-702.

CHAPTER IV. DISCUSSION

The ability to selectively activate and inhibit FcγRs is an important goal of immunology and medicine. In this dissertation, the analysis of FcγR activation at a single molecule level provided an improved understanding of the mechanisms of FcγR activation and inhibition that have implications for immunity and autoimmune pathogenesis and suggests new immunotherapeutic strategies.

From studying plasma membrane topography near sites of FcγR activation, it was found that the macrophage membrane remains close to its target in regions of FcγR ligation followed by a transition in topography to more vertical and more distal membrane in regions occupied by the $\alpha_M\beta_2$ integrin. Rather than tiptoeing at the sights of FcγR engagement with antibody, as was expected, and curving sharply to accommodate encroaching phosphatases, actin pushes the lamellipodia laterally from the point of contact, leaving a flat, but elevated plasma membrane in the wake of the advancing edge. Given that all phosphatases, like CD45 can deactivate FcγRs by diffusion driven collisions with FcγR clusters [1], we predicted that changes in the macrophage membrane topography would be adjacent to the target to help exclude proteins with large extracellular domains. Furthermore, this mechanism is likely to be of high importance when the antigen is mobile and on a deformable surface such as that found on ADCP targets.

Our findings provide some evidence that although integrins were not at the leading edge of the lamellipodia, $\alpha_M\beta_2$ podosomes may contribute to the macrophage phagocytic cup [1, 2], however the ligand and mode of activation remains undefined. A

typical diagnostic of integrin activation, talin and vinculin accumulate at podosomes formed against IgG-coated glass [2]. Thus, the arrangements of $\alpha_M\beta_2$ are overall consistent with this model.

However, evidence contradicting this model includes the fact that $\alpha_M\beta_2$, talin and vinculin were not found to be significant hits in our phagocytic screen. Thus, specific integrins and the general activating machinery does not seem to be required. In support of the podosome hypothesis was the observation that the actin nucleators and their adaptors, Arp 2/3 and WAVE2 were found to be very important by our whole genome screen. Of these, this work in this dissertation found new evidence that *Wasf2* and *Nckap1l*, genes coding for members of the WAVE2 complex, control the organization of the FcγRs and are important for establishing the leading-edge dynamics of the pseudopod. Surprisingly, *Was*, the gene coding for WASP, was not needed for the lateral actin polymerization but was involved in controlling the organization of the FcγRs in contact with the target, potentially by regulating the activation of integrins in the post FcγR zone. At this point, it is unclear what the relationship between WASP activity and integrins is in organizing the phagocytic cup and its potential role in forming a diffusional barrier between CD45 phosphatases and the FcγR clusters [1]. These findings provide a new line of investigation for delineating the divergent roles of the WASP and WAVE2 machineries in regulating FcγR signaling and phagocytic function.

Future work on the role of WAVE2 in the engulfment of phagocytic targets will be needed to delineate how WAVE2 regulates FcγR clustering. Polarized TIRF experiments of knockout macrophages will delineate the effects of WAVE2 and WASP on the membrane topography and contributions of integrins to shaping FcγR clustering

and activation. We propose that the lateral actin polymerization is mediated by WAVE2 recruitment of Arp2/3 at the periphery of the phagosome, driving the lamellipodia forward and that this facilitates clustering of FcγR and flattening of the plasma membrane against the target as it advances. Additionally, correlation of polTIRF with fluorescently tagged actin, integrins, and the WAVE2 components in mutant macrophages would allow testing of this hypothesis.

This dissertation also addressed FcγR activation regarding receptor valency by comparing the cell surface dynamics, internalization, and Syk kinase recruitment to engineered Fc molecules. In order to design an inhibitor for IgG-mediated autoimmune diseases, the question of receptor valency was addressed by Ortiz et. al. by designing multivalent Fc molecules [3]. They successfully identified a pentameric agonist for receptor activation and a trimer that potently inhibited activation. By utilizing multivalent Fc molecules, we found that small pentameric FcγR clusters are internalized and recruit Syk to endosomes. This finding is significant for the field of immunology because it provides evidence of a unique form of FcγR activation that may occur in some autoimmune diseases where immune complexes form with small, soluble antigen. Additionally, it provides insights that are valuable for inhibition strategies. The trimeric Fc, SIF1, is a potent inhibitor in animal autoimmune models, and is moving on to clinical trials [3]. Until recently, its route of inhibition was not understood, however our findings demonstrate that SIF1 precludes endocytosis, behaving like a single receptor, while docking three FcγRs. With its high avidity for the FcγR, it makes an ideal inhibitor.

Future work for this project includes investigation of FcγR endocytosis and activation on endosomes. It is not clear if clusters larger than five will always promote

activation on endosomes or if the geometry is particularly important. This could be tested by using some of the larger multivalent Fc molecules designed by Momenta Pharmaceutical [3]. A simple way to determine if PentX clusters promote endocytosis would be to inhibit endocytosis with drugs such as Pitstop and Dynasore, which arrest clathrin mediated endocytosis. Additionally, mutagenesis of the predicted motifs that signal for endocytosis would be key in determining the mechanism of endocytosis.

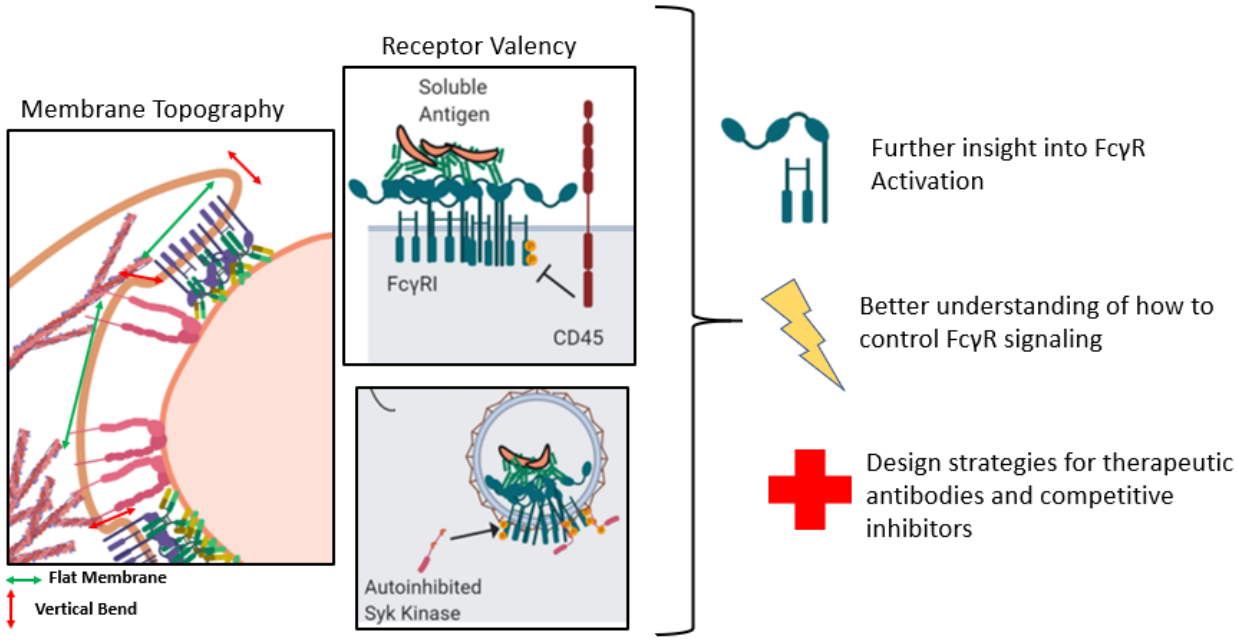

Figure 4.1 Models described in this dissertation provide insights into FcγR activation and signaling that may be valuable in designing therapeutic strategies. (Created with BioRender)

From FcγR clustering and signaling for phagocytosis, to small, mobile FcγR clusters driving responses to ICs, the FcγR plays an expansive role in the immune system. Understanding the nanoscale details of FcγR clustering and membrane topography provides new insights into the mechanisms by which FcγR clustering controls activation and provides strategies for inhibition (Fig. 4.1). This dissertation provides a new insight

into these processes and provides a roadmap for understanding the contributions of the newly discovered molecular machinery involved in FcγR activation.

References

1. Freeman, S.A., et al., *Integrins Form an Expanding Diffusional Barrier that Coordinates Phagocytosis.* Cell, 2016. **164**(1-2): p. 128-140.
2. Ostrowski, P.P., et al., *Dynamic Podosome-Like Structures in Nascent Phagosomes Are Coordinated by Phosphoinositides.* Dev Cell, 2019. **50**(4): p. 397-410 e3.
3. Ortiz, D.F., et al., *Elucidating the interplay between IgG-Fc valency and FcγR activation for the design of immune complex inhibitors.* Science Translational Medicine, 2016. **8**(365): p. 365ra158.